arXiv:1211.3322v1 [cs.IT] 14 Nov 2012

The Degrees of Freedom Region of Temporally-Correlated MIMO Networks with Delayed CSIT

Xinping Yi, *Student Member, IEEE*, Sheng Yang, *Member, IEEE*,
David Gesbert, *Fellow, IEEE*, Mari Kobayashi, *Member, IEEE*

Abstract

We consider the temporally-correlated Multiple-Input Multiple-Output (MIMO) broadcast channel (BC) and interference channel (IC) where the transmitters have (i) *delayed* channel state information (CSI) obtained from a latency-prone feedback channel as well as (ii) imperfect *current* CSIT, obtained, e.g., from prediction on the basis of these past channel samples. The degrees of freedom (DoF) regions for certain (important) cases of the two-user broadcast and interference MIMO networks under such conditions are characterized. The proposed DoF achieving schemes exploit a particular combination of the space-time alignment protocol (referred to as MAT alignment) designed for fully outdated CSIT feedback channels together with the use of approximate zero-forcing (ZF) precoders. The design strategies build and extend upon recently reported techniques for the MISO BC, using compressing and forwarding of the residual interference left after the approximate ZF precoding in a digital fashion.

I. INTRODUCTION

While the capacity region of the Multiple-Input Multiple-Output (MIMO) broadcast channel (BC) was established in [1], the characterization of the capacity of Gaussian interference channel (IC) has been a long-standing open problem, even for the two-user single-antenna case. Recent progress sheds light on this problem from various perspectives, among which the authors in [2] characterized the degrees of freedom (DoF) region, specializing to the large SNR regime, for the two-user MIMO IC. Such advance nevertheless suggests achievable schemes which require the full knowledge of channel state information (CSI) at both the transmitter and receiver sides. In practice, however, the acquisition of perfect CSI at the transmitters is difficult, if not impossible, especially for fast fading channels. The

X. Yi and D. Gesbert are with the Mobile Communications Dept., EURECOM, 06560 Sophia Antipolis, France (email: {xinping.yi, david.gesbert}@eurecom.fr).

S. Yang and M. Kobayashi are with the Telecommunications Dept., SUPELEC, 91190 Gif-sur-Yvette, France (e-mail: {sheng.yang, mari.kobayashi}@supelec.fr).

This work has been performed in the framework of the European research projects HARP (FP7 ICT Objective 1.1) and HIATUS (FET-Open grant number: 265578), as well as the French ANR project FIREFLIES (ANR-10-INTB-0302).

This work was presented in part at Asilomar Conference on Signals and Systems 2012, Pacific Grove, CA.

CSIT obtained via feedback suffers from delays, which renders the available CSIT feedback possibly fully obsolete (i.e., uncorrelated with the current true channel) under the fast fading channel and, seemingly non-exploitable in view of designing the spatial precoding. Recently, the impact of feedback delays in such scenario (referred to as "delayed CSIT") was considered in [3] for the MISO BC, and a scheme termed here as *MAT alignment* was proposed. The key contribution in [3] was to establish the usefulness of even completely outdated channel state information in designing precoders achieving strictly better DoF than what is obtained without any CSIT. The essential ingredient for the proposed scheme in [3] lies in the use of a multi-slot protocol initiating with the transmission of unprecoded information symbols to the user terminals, followed by the *analog* forwarding of the interference overheard in the previous time slots. Most recently, generalizations under the similar principle to the MIMO BC [4] and MIMO IC [5, 6] settings were also addressed, again establishing DoF strictly beyond the ones obtained without CSIT [7–9] but below the ones with perfect CSIT [2].

Albeit inspiring and fascinating in nature, these works made the assumption that the delayed CSIT bears no correlation with the current channel realization. Hence, these results pessimistically consider that no estimate for the *current* channel realization is producible to the transmitter. Owing to the finite Doppler spread behavior of fading channels, it is however the case in many real life situations that the past channel realizations can provide *some* information about the current one. Therefore a scenario where the transmitter is endowed with delayed CSI in addition to some (albeit imperfect) estimate of the current channel is of practical relevance. This form of combined perfect delayed and imperfect current CSIT was first introduced in [10] for the MISO BC whereby a novel transmission scheme was proposed which improves over pure MAT alignment in constructing precoders based on delayed *and* current CSIT estimate. The full characterization of the optimal DoF for the hybrid CSIT was reported in [11, 12] for MISO BC and in [13] for MISO IC. The key idea behind the schemes in [10–13] lies in the modification of the MAT protocol where i) the initial time slot involves transmission of *precoded* symbols, followed by the forwarding of *residual* interference overheard in the first time slot, and ii) the taking advantage of the reduced power for the residual interference (compared with full power interference in MAT) based on a suitable *quantization* method.

In this paper, we extend the results in [10, 11, 13] and consider the two-user temporally-correlated MIMO networks both for the BC and IC cases. Note that the generalization from MISO to MIMO networks is unfortunately not a trivial step. The additional spatial dimension at the receiver side enables to cancel a certain amount of residual interference (generated by the impreciseness of transmit precoding) and thus intuitively is expected to enhance the achievable DoF, especially for larger number of transmit than receive antennas. Furthermore, the clarity of the description of DoF achieving schemes in MIMO settings is hampered by the enumeration of all possible antenna configurations resulting in slightly different transmission strategies as was noted previously for the purely delayed CSIT case [5, 6]. A similar issue arises here and, indeed, working out the full DoF region for an arbitrary MIMO network appears difficult at this stage. In order to ease exposition, we choose to focus on one important particular scenario offered by so-called *symmetric* networks where nodes have the same number of transmit (M) and receive (N) antennas, with possible $M \neq N$. Overall, our results allow to bridge between previously reported CSIT scenarios such as the pure delayed CSIT of [3–6] and the pure instantaneous CSIT scenarios for the MIMO setting. We tackle both the BC and IC configurations as we point out the tight connection between the DoF achieving transmission strategies in both these settings.

More specifically, we obtain the following key results:

- We establish outer bounds on the DoF region for the two-user temporally-correlated MIMO BC and IC with perfect delayed plus imperfect current CSIT, as a function of the current CSIT quality *exponent*. By introducing a virtual received signal for IC, we link the outer bound of IC nicely to that of BC, arriving at the same outer bound result for both cases. In addition to the genie-aided bounding techniques and the application of the extremal inequality in [10, 11, 13], we develop a set of upper and lower bounds of ergodic capacity for MIMO channels, which is essential for the MIMO case but not extendable from MISO.
- We propose schemes which achieve the key vertices of the outer bound region with perfect delayed plus imperfect current CSIT. The schemes build on the principles of a time-slotted protocol, starting with the spatial zero-forcing (ZF) precoded transmission of information symbols from the transmitter(s) simultaneously and followed by forwarding of the residual interferences in a *compressed* fashion. In particular, the MIMO BC/IC with $M=3$ and $N=2$ achieves sum DoF $\left(\frac{12+3\alpha}{5}\right)$. This smoothly bridges two special cases: the case with pure delayed CSIT ($\alpha=0$) and that with perfect current CSIT ($\alpha=1$).

It is worth noting that our results embrace the previously reported particular cases: the perfect CSIT setting [2] (i.e., current CSIT of perfect quality), the pure delayed CSIT setting [5, 6] (i.e., current CSIT of zero quality), and the special MISO case [10, 11, 13] with $N=1$.

Notation: Matrices and vectors are represented as uppercase and lowercase letters, and matrix transport, Hermitian transport, inverse and determinant are denoted by $\boldsymbol{A}^{\mathsf{T}}$, $\boldsymbol{A}^{\mathsf{H}}$, $\boldsymbol{A}^{-1}$ and $\det(\boldsymbol{A})$, respectively. $\boldsymbol{h}^{\perp}$ is the normalized orthogonal component of any nonzero vector $\boldsymbol{h}$. The approximation $f(P) \sim g(P)$ is in the sense of $\lim_{P\to\infty} \frac{f(P)}{g(P)} = C$, where $C>0$ is a constant that does not scale as P. Partial ordering of Hermitian matrices is denoted by $\succeq$ and $\preceq$, i.e., $\boldsymbol{A} \preceq \boldsymbol{B}$ means $\boldsymbol{B}-\boldsymbol{A}$ is positive semidefinite. Logarithms are in base 2 and e for $\log$ and $\ln$, respectively. $\doteq$, $\dot{\leq}$ and $\dot{\geq}$ are in the sense of large P.

II. SYSTEM MODEL

A. Two-user MIMO Broadcast Channel

For a symmetric two-user (M,N) MIMO broadcast channel (BC) with M antennas at the transmitter and N antennas at each receiver, the discrete time signal model is given by

$$\boldsymbol{y}_i(t) = \boldsymbol{H}_i(t)\boldsymbol{x}(t) + \boldsymbol{z}_i(t) \tag{1a}$$

for any time instant t, where $\boldsymbol{H}_i(t) \in \mathbb{C}^{N\times M}$ is the channel matrix for i-th receiver ($i=1,2$); $\boldsymbol{z}_i(t) \sim \mathcal{N}_{\mathbb{C}}\left(0, \mathbf{I}_N\right)$ is the normalized AWGN vector at the respective receiver and is independent of channel matrices and transmitted signals; the coded input signal $\boldsymbol{x}(t) \in \mathbb{C}^{M\times 1}$ is subject to the power constraint $\mathbb{E}\|\boldsymbol{x}(t)\|^2 \leq P$, $\forall\, t$. Denote by $\boldsymbol{H}_{i[k_1:k_2]}(t)$ the submatrix of $\boldsymbol{H}_i(t)$ from k_1-th row to k_2-th row ($k_1 \leq k_2$). Define $\boldsymbol{H}(t) \triangleq \{\boldsymbol{H}_1(t), \boldsymbol{H}_2(t)\}$ as the ensemble of channel matrices.

B. Two-user MIMO Interference Channel

For a symmetric two-user (M, N) MIMO interference channel (IC) with M antennas at each transmitter and N antennas at each receiver, the discrete time signal model is given by

$$\boldsymbol{y}_i(t) = \boldsymbol{H}_{i1}(t)\boldsymbol{x}_1(t) + \boldsymbol{H}_{i2}(t)\boldsymbol{x}_2(t) + \boldsymbol{z}_i(t) \tag{2a}$$

for any time instant t, where $\boldsymbol{H}_{ji}(t) \in \mathbb{C}^{N \times M}$ $(i, j = 1, 2)$ is the channel matrix between Tx-i and Rx-j; the coded input signal $\boldsymbol{x}_i(t) \in \mathbb{C}^{M \times 1}$ is subject to the power constraint $\mathbb{E}\|\boldsymbol{x}_i(t)\|^2 \leq P$, $\forall\, t$. Denote by $\boldsymbol{H}_{ikj}(t)$ the k-th row of $\boldsymbol{H}_{ij}(t)$ and $\boldsymbol{H}_{i[k_1:k_2]j}(t)$ as the submatrix of $\boldsymbol{H}_{ij}(t)$ from k_1-th row to k_2-th row $(k_1 \leq k_2)$. Define $\boldsymbol{H}(t) \triangleq \{\boldsymbol{H}_{11}(t), \boldsymbol{H}_{21}(t), \boldsymbol{H}_{12}(t), \boldsymbol{H}_{22}(t)\}$.

For notational brevity, we hereafter refer to (M, N) MIMO BC and IC as (M, N) MIMO network, and define $\boldsymbol{H}^k \triangleq \{\boldsymbol{H}(t)\}_{t=1}^k$, and $\hat{\boldsymbol{H}}^k \triangleq \{\hat{\boldsymbol{H}}(t)\}_{t=1}^k$, where $k = 1, \cdots, n$.

C. Assumptions

Assumption 1 (fading channel)**.** *At any given time instant t, the element of channel matrix $\boldsymbol{H}_i(t)$ (resp. $\boldsymbol{H}_{ij}(t)$) is drawn from a stationary and ergodic random process, and any concatenated matrix with rows extracted from $\boldsymbol{H}_i(t)$ (resp. $\boldsymbol{H}_{ij}(t)$) is full rank almost surely.*

Assumption 2 (perfect delayed CSIT and imperfect current CSIT)**.** *At each time instant t, the transmitter knows perfectly the delayed CSI $\boldsymbol{H}^{t-1}$, and obtains an imperfect estimate of the current CSI $\hat{\boldsymbol{H}}(t)$, which could, for instance, be produced by standard prediction based on past samples. The current CSIT estimate is modeled by*

$$\boldsymbol{H}(t) = \hat{\boldsymbol{H}}(t) + \tilde{\boldsymbol{H}}(t) \tag{3}$$

where the estimate $\hat{\boldsymbol{H}}(t)$ and estimation error $\tilde{\boldsymbol{H}}(t)$ are independent, and $\tilde{\boldsymbol{H}}(t)$ is independent and identically distributed (i.i.d.) with each entry being assumed to be zero-mean and with variance $(1 - \sigma^2)$, σ^2, respectively ($0 \leq \sigma^2 \leq 1$). Further, we assume the following Markov chain

$$(\boldsymbol{H}^{t-1}, \hat{\boldsymbol{H}}^{t-1}) \rightarrow \hat{\boldsymbol{H}}^t \rightarrow \boldsymbol{H}^t, \quad \forall t, \tag{4}$$

which means $\boldsymbol{H}^t$ is independent of $(\boldsymbol{H}^{t-1}, \hat{\boldsymbol{H}}^{t-1})$ conditional on $\hat{\boldsymbol{H}}^t$.

Assumption 3 (perfect delayed/current CSIR, and imperfect current CSI at the receiver)**.** *At each time instant t, the receivers know perfectly the delayed/current CSI and somehow know the same imperfect current CSI at the transmitter both up to instant t for all links, i.e., $\boldsymbol{H}^t$ and $\hat{\boldsymbol{H}}^t$.*

Assumption 3 is in accordance with previous works with delayed CSIT, and since linear prediction can be applied at the receiver side as well to produce current channel estimate. It does not add any limitation over the assumption made in [3–5]. We point out that only local CSIT/CSIR (the channel links with which the node is connected) is really helpful and leads to the same result. Nevertheless, we assume the CSIT/CSIR to be available in a global fashion for presentation simplicity.

We assume that the estimation error σ^2 can be parameterized as an exponential function of the power P, so that we can characterize the DoF region of MIMO networks with respect to this exponent. To this end, we introduce a parameter $\alpha \geq 0$, such that

$$\alpha \triangleq - \lim_{P \to \infty} \frac{\log \sigma^2}{\log P}. \tag{5}$$

This α indicates the quality of current CSIT at high SNR. While $\alpha = 0$ reflects the case with no current CSIT, $\alpha \to \infty$ corresponds to that with perfect instantaneous CSIT. As a matter of fact, when $\alpha \geq 1$, the quality of the imperfect current CSIT is sufficient to avoid the DoF loss, and ZF precoding with this imperfect CSIT is able to achieve the maximum DoF [14]. Therefore, we focus on the case $\alpha \in [0, 1]$ henceforth. The connections between the above model and the linear prediction over existing time-correlated channel models with prescribed user mobility are highlighted in [10, 15]. According to the definition of the estimated current CSIT, we have $\mathbb{E}|\boldsymbol{h}^{\mathsf{H}}(t)\hat{\boldsymbol{h}}^{\perp}(t)|^2 = \sigma^2 \sim P^{-\alpha}$, with $\boldsymbol{h}$ representing any column of channel matrices, and $\hat{\boldsymbol{h}}$ being its corresponding estimate.

III. MAIN RESULTS ON THE DEGREES OF FREEDOM REGION

A rate pair (R_1, R_2) is said to be achievable for the two-user MIMO networks with perfect delayed CSIT and imperfect current CSIT if there exists a $\left(2^{nR_1}, 2^{nR_2}, n\right)$ code scheme consists of:

- two message sets $\mathcal{W}_1 \triangleq [1 : 2^{nR_1}]$ and $\mathcal{W}_2 \triangleq [1 : 2^{nR_2}]$, from which two independent messages W_1 and W_2 intended respectively to the Rx-1 and Rx-2 are uniformly chosen;
- one encoding function for (each) transmitter:

$$\begin{aligned} &\text{BC:} \quad \boldsymbol{x}(t) = f_t\left(W_1, W_2, \boldsymbol{H}^{t-1}, \hat{\boldsymbol{H}}^t\right) \\ &\text{IC:} \quad \boldsymbol{x}_i(t) = f_{i,t}\left(W_i, \boldsymbol{H}^{t-1}, \hat{\boldsymbol{H}}^t\right), \ i = 1, 2; \end{aligned} \tag{6a}$$

- and one decoding function at the corresponding receiver,

$$\hat{W}_j = g_j\left(\boldsymbol{Y}_j^n, \boldsymbol{H}^n, \hat{\boldsymbol{H}}^n\right), \ j = 1, 2 \tag{7}$$

  for the Rx-j, where $\boldsymbol{Y}_j^n \triangleq \{\boldsymbol{y}_j(t)\}_{t=1}^n$,

such that the average decoding error probability $P_e^{(n)}$, defined as $P_e^{(n)} \triangleq \mathbb{E}_{W_1 \in \mathcal{W}_1, W_2 \in \mathcal{W}_2} \mathbb{P}\left((W_1, W_2) \neq (\hat{W}_1, \hat{W}_2)\right)$, vanishes as the code length n tends to infinity. The capacity region $\mathcal{C}$ is defined as the set of all achievable rate pairs. Accordingly, the DoF region can be defined as follows:

Definition 1 (the degrees of freedom region)**.** *The degrees of freedom (DoF) region for the two-user MIMO network is defined as*

$$\mathcal{D} = \left\{ (d_1, d_2) \in \mathbb{R}_+^2 | \ \forall (w_1, w_2) \in \mathbb{R}_+^2, w_1 d_1 + w_2 d_2 \leq \limsup_{P \to \infty} \left(\sup_{(R_1, R_2) \in \mathcal{C}} \frac{w_1 R_1 + w_2 R_2}{\log P} \right) \right\}. \tag{8}$$

Accordingly, the main results of this paper are stated as the following three theorems:

Theorem 1 (outer bound)**.** *For the two-user* (M,N) *MIMO network with perfect delayed and imperfect current CSIT, the DoF pair* $(d_1,d_2)\in\mathbb{R}_+^2$ *is outer-bounded by*

$$d_1 \le \min\{M,N\}, \tag{9a}$$

$$d_2 \le \min\{M,N\}, \tag{9b}$$

$$\frac{d_1}{\min\{M,N\}}+\frac{d_2}{\min\{M,2N\}} \le 1+\frac{\min\{M,2N\}-\min\{M,N\}}{\min\{M,2N\}}\alpha, \tag{9c}$$

$$\frac{d_1}{\min\{M,2N\}}+\frac{d_2}{\min\{M,N\}} \le 1+\frac{\min\{M,2N\}-\min\{M,N\}}{\min\{M,2N\}}\alpha, \tag{9d}$$

$$\textit{for BC:}\quad d_1+d_2 \le \min\{M,2N\}, \tag{9e}$$

$$\textit{for IC:}\quad d_1+d_2 \le \min\{2M,2N,\max\{M,N\}\}, \tag{9f}$$

where α *is the current CSIT quality exponent.*

Proof: Note that the first two bounds hold because the DoF of the point-to-point (M,N) MIMO channel is upper bounded by $\min\{M,N\}$, and the sum DoF outer bounds (9e)-(9f) are from BC/IC with perfect CSIT setting [1,2], which should hold also for our setting. Hence, it is sufficient to prove bounds (9c) and (9d), which are provided in Section IV. ■

Remark: Interestingly, when $M \ge N$, the sum DoF outer bounds of BC and IC coincide with $d_1+d_2 \le \min\{M,2N\}$, and hence both BC and IC hold the same DoF outer bounds. Nevertheless, these sum DoF bounds are inactive when $M \ge N$ as will be detailed below.

Theorem 2 (tightness for the $M \le N$ and $M \ge 2N$ cases)**.** *For the two-user* (M,N) *MIMO network with perfect delayed and imperfect current CSIT, the above outer bound of DoF region is tight when* $M \le N$ *and* $M \ge 2N$*.*

Proof: The outer bounds can be deduced from (9) and the achievable schemes are in Section V. A and V. C. ■

Remark:

- When $M \le N$, the DoF regions with no CSIT, with delayed CSIT and with perfect CSIT are identical [5, 7–9], i.e., the weighted sum DoF bounds (9c)-(9d) are inactive, showing additional CSIT does not improve DoF region.
- When $M \ge 2N$, for (M,N) MIMO network with perfect delayed and imperfect current CSIT, the optimal DoF region can be characterized by

$$d_1 \le N, \tag{10a}$$

$$d_2 \le N, \tag{10b}$$

$$d_1+2d_2 \le N(2+\alpha), \tag{10c}$$

$$2d_1+d_2 \le N(2+\alpha), \tag{10d}$$

which is N times enlarged of the MISO case [11,13]. Note that the sum DoF bounds (9e)-(9f) are inactive and redundant. For illustration, the DoF region is provided in Fig. 1. Those with pure perfect delayed CSIT (black), and perfect instantaneous CSIT (dashed black) are also plotted for the comparison purpose. It shows that the DoF region in our setting is strictly larger than that with pure delayed CSIT and approaches the region with perfect CSIT as the quality of current CSIT increases.

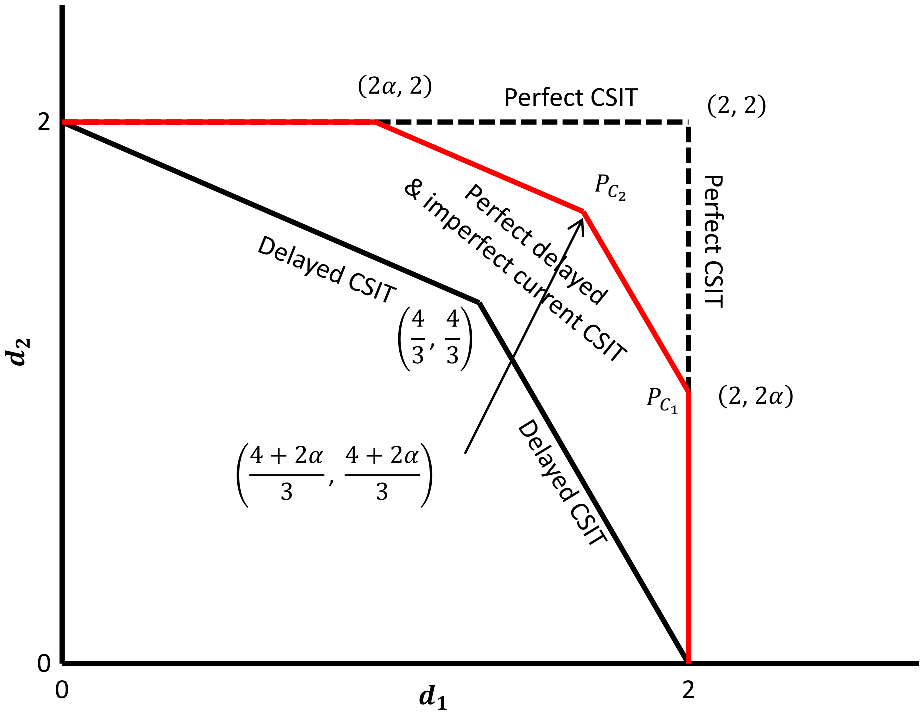

Fig. 1: The optimal DoF region for the two-user MIMO network (e.g., $M = 4$, $N = 2$, and $\alpha = 0.5$).

Theorem 3 (inner bound for the $N < M < 2N$ case)**.** *For the two-user (M, N) MIMO network with perfect delayed and imperfect current CSIT, the DoF region*

$$d_1 \leq N, \tag{11a}$$

$$d_2 \leq N, \tag{11b}$$

$$\frac{d_1}{N} + \frac{d_2}{M} \leq 1 + \frac{M-N}{M}\alpha, \tag{11c}$$

$$\frac{d_1}{M} + \frac{d_2}{N} \leq 1 + \frac{M-N}{M}\alpha, \tag{11d}$$

$$d_1 + d_2 \leq \frac{2MN + M(M-N)\alpha}{M+N}, \tag{11e}$$

is achievable for the case when $N < M < 2N$.

Proof: The necessary condition of the inner bounds (11a)-(11d) can be deduced from (9), while the sum DoF inner bound (11e) inactivates the sum DoF outer bounds (9e)-(9f), and the sufficient condition (i.e., the achievability) is provided in Section V. B. ■

Take $(3, 2)$ MIMO network for instance. The achievable DoF region with mixed delayed and imperfect current CSIT (red) is provided in Fig. 2. The DoF regions with pure perfect delayed CSIT (black), perfect CSIT (dashed black) and also the outer bound (dashed red) are also plotted for comparison. Compared to the outer bound, the achievable DoF region is further bounded by a sum DoF constraint (cf. (11e)).

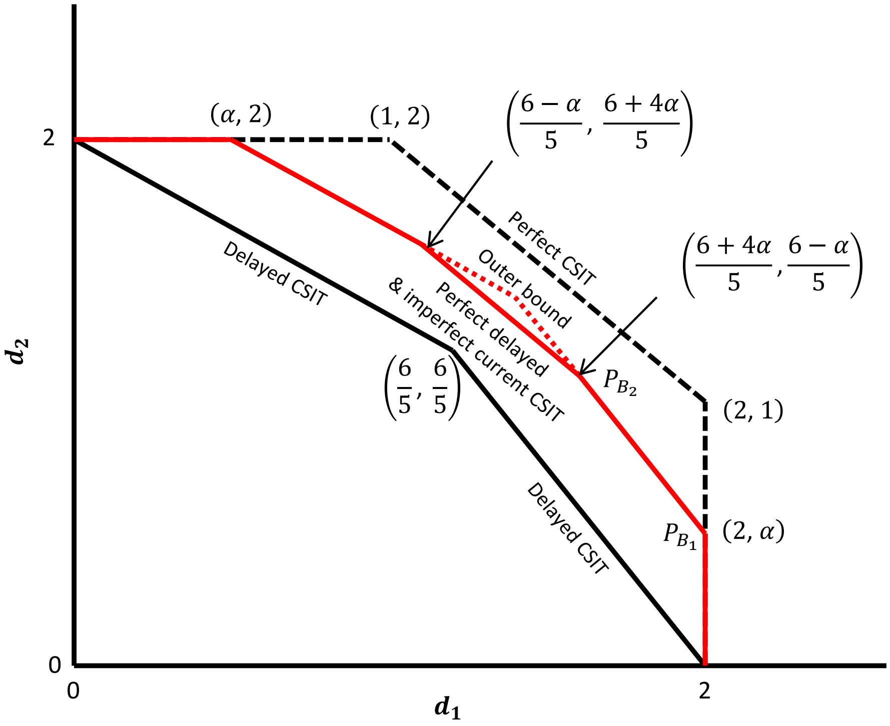

Fig. 2: The achievable DoF region for two-user (M, N) MIMO networks (e.g., $M = 3$, $N = 2$, and $\alpha = 0.5$).

Notice that the achievable DoF region is subsumed in the outer bounds, whose sum DoF bound has not yet been proven. We conjecture that such achievable scheme is optimal, since it smoothly bridges two extreme cases when $\alpha = 0$ and $\alpha = 1$.

IV. PROOFS FOR THE OUTER BOUND

To obtain the outer bounds, the following ingredients are essential:

- *Genie-aided* bounding techniques by providing side information of one receiver to the other one [5];
- *Extremal inequality* to bound the weighted difference of conditional differential entropies [16];
- *Ergodic capacity upper and lower bounds* for MIMO channels [17, 18].

We first provide the outer bounds by employing the genie-aided techniques for BC and IC, respectively, reaching the similar formulation of the rate bounds. With the help of extremal inequalities, the weighted sum rates are further bounded. Finally, the bounds in terms of α are arrived by applying the ergodic capacity bounds of MIMO channels. Note that we consider only the case of $M \geq N$ in this section since the DoF results for $M \leq N$ coincide with the no CSIT case and are already known [7–9].

A. Genie-aided Bounding Techniques

To obtain the outer bounds, we adopt a genie-aided upper bounding technique reminisced in [4, 5], by providing Rx-2 the side information of the Rx-1's message W_1 as well as received signal $\boldsymbol{Y}_1^n$. As stated in Assumption 3, both receivers know the CSI $\boldsymbol{H}(t)$ perfectly and instantaneously as well as the imperfect current CSI $\hat{\boldsymbol{H}}(t)$ at time t.

For notational brevity, we define a virtual received signal as

$$\bar{\boldsymbol{y}}_i(t) \triangleq \begin{cases} \boldsymbol{H}_i(t)\boldsymbol{x}(t) + \boldsymbol{z}_i(t) & \text{for BC} \\ \boldsymbol{H}_{i2}(t)\boldsymbol{x}_2(t) + \boldsymbol{z}_i(t) & \text{for IC} \end{cases} \tag{12}$$

and we also define $\boldsymbol{X}^n \triangleq \{\boldsymbol{x}(t)\}_{t=1}^n$, $\boldsymbol{X}_i^n \triangleq \{\boldsymbol{x}_i(t)\}_{t=1}^n$, $\boldsymbol{Y}_i^k \triangleq \{\boldsymbol{y}_i(t)\}_{t=1}^k$, and $\bar{\boldsymbol{Y}}_i^k \triangleq \{\bar{\boldsymbol{y}}_i(t)\}_{t=1}^k$. Denote also $n\epsilon_n \triangleq 1 + nRP_e^{(n)}$ where ϵ_n tends to zero as $n \to \infty$ by the assumption that $\lim_{n\to\infty} P_e^{(n)} = 0$.

1) Broadcast Channel: The genie-aided model is a degraded BC $\boldsymbol{X}^n \to (\boldsymbol{Y}_1^n, \boldsymbol{Y}_2^n) \to \boldsymbol{Y}_1^n$, and therefore we bound the achievable rates by applying Fano's inequality as

$$\begin{aligned}
n(R_1 - \epsilon_n) &\leq I(W_1; \boldsymbol{Y}_1^n | \boldsymbol{H}^n, \hat{\boldsymbol{H}}^n) && (13) \\
&= \sum_{t=1}^n I(W_1; \boldsymbol{y}_1(t) | \boldsymbol{H}^n, \hat{\boldsymbol{H}}^n, \boldsymbol{Y}_1^{t-1}) + n\epsilon_n && (14) \\
&= \sum_{t=1}^n \Big(h(\boldsymbol{y}_1(t) | \boldsymbol{H}^n, \hat{\boldsymbol{H}}^n, \boldsymbol{Y}_1^{t-1}) - h(\boldsymbol{y}_1(t) | \boldsymbol{H}^n, \hat{\boldsymbol{H}}^n, \boldsymbol{Y}_1^{t-1}, W_1) \Big) && (15) \\
&\leq \sum_{t=1}^n h(\boldsymbol{y}_1(t) | \boldsymbol{H}(t)) - h(\boldsymbol{y}_1(t) | \mathcal{U}(t), \boldsymbol{H}(t)) && (16) \\
&\leq nN \log P - \sum_{t=1}^n h(\bar{\boldsymbol{y}}_1(t) | \mathcal{U}(t), \boldsymbol{H}(t)) + n \cdot O(1) && (17) \\
n(R_2 - \epsilon_n) &\leq I(W_2; \boldsymbol{Y}_1^n, \boldsymbol{Y}_2^n, W_1 | \boldsymbol{H}^n, \hat{\boldsymbol{H}}^n) && (18) \\
&= I(W_2; \boldsymbol{Y}_1^n, \boldsymbol{Y}_2^n | W_1, \boldsymbol{H}^n, \hat{\boldsymbol{H}}^n) && (19) \\
&= \sum_{t=1}^n I(W_2; \boldsymbol{y}_1(t), \boldsymbol{y}_2(t) | \boldsymbol{H}^n, \hat{\boldsymbol{H}}^n, \boldsymbol{Y}_1^{t-1}, \boldsymbol{Y}_2^{t-1}, W_1) && (20) \\
&\leq \sum_{t=1}^n I(\boldsymbol{x}(t); \boldsymbol{y}_1(t), \boldsymbol{y}_2(t) | \boldsymbol{H}^n, \hat{\boldsymbol{H}}^n, \boldsymbol{Y}_1^{t-1}, \boldsymbol{Y}_2^{t-1}, W_1) && (21) \\
&= \sum_{t=1}^n \Big(h(\boldsymbol{y}_1(t), \boldsymbol{y}_2(t) | \boldsymbol{H}^n, \hat{\boldsymbol{H}}^n, \boldsymbol{Y}_1^{t-1}, \boldsymbol{Y}_2^{t-1}, W_1) && (22) \\
&\qquad\qquad - h(\boldsymbol{y}_1(t), \boldsymbol{y}_2(t) | \boldsymbol{x}(t), \boldsymbol{H}^n, \hat{\boldsymbol{H}}^n, \boldsymbol{Y}_1^{t-1}, \boldsymbol{Y}_2^{t-1}, W_1) \Big) && (23)
\end{aligned}$$

$$\leq \sum_{t=1}^{n} h(\boldsymbol{y}_1(t), \boldsymbol{y}_2(t)|\boldsymbol{H}^n, \hat{\boldsymbol{H}}^n, \boldsymbol{Y}_1^{t-1}, \boldsymbol{Y}_2^{t-1}, W_1) \quad (24)$$

$$= \sum_{t=1}^{n} h(\bar{\boldsymbol{y}}_1(t), \bar{\boldsymbol{y}}_2(t)|\mathcal{U}(t), \boldsymbol{H}(t)) \quad (25)$$

where $\mathcal{U}(t) \triangleq \left\{\bar{\boldsymbol{Y}}_1^{t-1}, \bar{\boldsymbol{Y}}_2^{t-1}, \boldsymbol{H}^{t-1}, \hat{\boldsymbol{H}}^t, W_1\right\}$, (16) is from (12) and because (a) conditioning reduces differential entropy, and (b) $\{\bar{\boldsymbol{y}}_1(t), \bar{\boldsymbol{y}}_2(t)\}$ are independent of $\boldsymbol{H}_{t+1}^n$ and $\hat{\boldsymbol{H}}_{t+1}^n$; (17) follows the fact that the rate of the point-to-point $M \times N$ MIMO channel (i.e., between Tx an Rx-1) with $M \geq N$ is bounded by $nN \log P + n \cdot O(1)$; (19) is due to the independence between W_1 and W_2; (21) follows date processing inequality; and (24) is obtained by noticing (a) translation does not change differential entropy, (b) Gaussian noise terms are independent from instant to instant, and are also independent of the channel matrices and the transmitted signals, and (c) the differential entropy of Gaussian noise is nonnegative.

2) Interference Channel: Given the message and corresponding channel, part of the received signal is deterministic and therefore removable without mutual information loss. Hence, similarly to the BC case, we formulate a degraded channel model, i.e., $\boldsymbol{X}_2^n \to \left(\bar{\boldsymbol{Y}}_1^n, \bar{\boldsymbol{Y}}_2^n\right) \to \bar{\boldsymbol{Y}}_1^n$. By applying Fano's inequality, the achievable rate of Rx-1 and Rx-2 can be bounded as

$$n(R_1 - \epsilon_n) \leq I(W_1; \boldsymbol{Y}_1^n|\boldsymbol{H}^n, \hat{\boldsymbol{H}}^n) \quad (26)$$

$$= I(W_1, W_2; \boldsymbol{Y}_1^n|\boldsymbol{H}^n, \hat{\boldsymbol{H}}^n) - I(W_2; \boldsymbol{Y}_1^n|W_1, \boldsymbol{H}^n, \hat{\boldsymbol{H}}^n) \quad (27)$$

$$\leq nN \log P - I(W_2; \boldsymbol{Y}_1^n|W_1, \boldsymbol{H}^n, \hat{\boldsymbol{H}}^n) + n \cdot O(1) \quad (28)$$

$$= nN \log P - h(\boldsymbol{Y}_1^n|W_1, \boldsymbol{H}^n, \hat{\boldsymbol{H}}^n) + h(\boldsymbol{Y}_1^n|W_1, W_2, \boldsymbol{H}^n, \hat{\boldsymbol{H}}^n) + n \cdot O(1) \quad (29)$$

$$= nN \log P - h(\boldsymbol{Y}_1^n|W_1, \boldsymbol{H}^n, \hat{\boldsymbol{H}}^n) + n \cdot O(1) \quad (30)$$

$$= nN \log P - h(\bar{\boldsymbol{Y}}_1^n|\boldsymbol{H}^n, \hat{\boldsymbol{H}}^n) + n \cdot O(1) \quad (31)$$

$$\leq nN \log P - \sum_{t=1}^{n} h(\bar{\boldsymbol{y}}_1(t)|\boldsymbol{H}^n, \hat{\boldsymbol{H}}^n, \bar{\boldsymbol{Y}}_1^{t-1}, \bar{\boldsymbol{Y}}_2^{t-1}) + n \cdot O(1) \quad (32)$$

$$= nN \log P - \sum_{t=1}^{n} h(\bar{\boldsymbol{y}}_1(t)|\mathcal{U}(t), \boldsymbol{H}(t)) + n \cdot O(1) \quad (33)$$

$$n(R_2 - \epsilon_n) \leq I(W_2; \boldsymbol{Y}_1^n, \boldsymbol{Y}_2^n, W_1|\boldsymbol{H}^n, \hat{\boldsymbol{H}}^n) \quad (34)$$

$$= I(W_2; \boldsymbol{Y}_1^n, \boldsymbol{Y}_2^n|W_1, \boldsymbol{H}^n, \hat{\boldsymbol{H}}^n) \quad (35)$$

$$= I(W_2; \bar{\boldsymbol{Y}}_1^n, \bar{\boldsymbol{Y}}_2^n|\boldsymbol{H}^n, \hat{\boldsymbol{H}}^n) \quad (36)$$

$$= \sum_{t=1}^{n} I(W_2; \bar{\boldsymbol{y}}_1(t), \bar{\boldsymbol{y}}_2(t)|\boldsymbol{H}^n, \hat{\boldsymbol{H}}^n, \bar{\boldsymbol{Y}}_1^{t-1}, \bar{\boldsymbol{Y}}_2^{t-1}) \quad (37)$$

$$\leq \sum_{t=1}^{n} I(\boldsymbol{x}_2(t); \bar{\boldsymbol{y}}_1(t), \bar{\boldsymbol{y}}_2(t)|\boldsymbol{H}^n, \hat{\boldsymbol{H}}^n, \bar{\boldsymbol{Y}}_1^{t-1}, \bar{\boldsymbol{Y}}_2^{t-1}) \quad (38)$$

$$= \sum_{t=1}^{n} \Big(h(\bar{\boldsymbol{y}}_1(t), \bar{\boldsymbol{y}}_2(t)|\boldsymbol{H}^n, \hat{\boldsymbol{H}}^n, \bar{\boldsymbol{Y}}_1^{t-1}, \bar{\boldsymbol{Y}}_2^{t-1}) \quad (39)$$

$$- h(\bar{\boldsymbol{y}}_1(t), \bar{\boldsymbol{y}}_2(t) | \boldsymbol{x}_2(t), \boldsymbol{H}^n, \hat{\boldsymbol{H}}^n, \bar{\boldsymbol{Y}}_1^{t-1}, \bar{\boldsymbol{Y}}_2^{t-1}) \Big) \tag{40}$$

$$\le \sum_{t=1}^{n} h(\bar{\boldsymbol{y}}_1(t), \bar{\boldsymbol{y}}_2(t) | \boldsymbol{H}^n, \hat{\boldsymbol{H}}^n, \bar{\boldsymbol{Y}}_1^{t-1}, \bar{\boldsymbol{Y}}_2^{t-1}) \tag{41}$$

$$= \sum_{t=1}^{n} h(\bar{\boldsymbol{y}}_1(t), \bar{\boldsymbol{y}}_2(t) | \mathcal{U}(t), \boldsymbol{H}(t)) \tag{42}$$

where $\mathcal{U}(t) \triangleq \left\{ \bar{\boldsymbol{Y}}_1^{t-1}, \bar{\boldsymbol{Y}}_2^{t-1}, \boldsymbol{H}^{t-1}, \hat{\boldsymbol{H}}^{t} \right\}$, (28) follows the fact that the mutual information at hand is upper bounded by the rate of the $2M \times N$ point-to-point MIMO channel by cooperating two transmitters, given by $nN \log P + n \cdot O(1)$; (30) is due to the fact that (a) transmitted signal $\boldsymbol{X}_i^n$ is a deterministic function of messages, $\boldsymbol{H}^n$, and $\hat{\boldsymbol{H}}^{n-1}$ as specified in (6), and (b) translation does change differential entropy; (31) and (36) are obtained because translation preserves differential entropy; (32) is because conditioning reduces differential entropy; (41) is because (a) translation does not change differential entropy, (b) Gaussian noise terms are independent from instant to instant, and are also independent of the channel matrices and the transmitted signals, and (c) the differential entropy of Gaussian noise is nonnegative; and (42) is obtained due to the independence $\{\bar{\boldsymbol{y}}_1(t), \bar{\boldsymbol{y}}_2(t)\}$ of $\boldsymbol{H}_{t+1}^n$ and $\hat{\boldsymbol{H}}_{t+1}^n$.

It is worth noting that BC and IC share the common structure of the achievable rate bounds, and therefore can be further bounded in a similar way. To avoid redundancy, we give the proof for IC, which can be straightforwardly extended to BC.

B. Extremal Inequalities

Define

$$\boldsymbol{S}(t) \triangleq \begin{bmatrix} \boldsymbol{H}_{12}(t) \\ \boldsymbol{H}_{22}(t) \end{bmatrix} \qquad \hat{\boldsymbol{S}}(t) \triangleq \begin{bmatrix} \hat{\boldsymbol{H}}_{12}(t) \\ \hat{\boldsymbol{H}}_{22}(t) \end{bmatrix} \qquad \boldsymbol{K}(t) \triangleq \mathbb{E}\{\boldsymbol{x}_2(t)\boldsymbol{x}_2^{\mathsf{H}}(t) | \mathcal{U}(t)\}. \tag{43}$$

Due to the fact that Gaussian input maximizes the weighted difference of two differential entropies under the covariance constraint [16], given two integers $p > 0$, $q > 0$, we have

$$\frac{1}{p} h(\bar{\boldsymbol{y}}_1(t), \bar{\boldsymbol{y}}_2(t) | \mathcal{U}(t), \boldsymbol{H}(t)) - \frac{1}{q} h(\bar{\boldsymbol{y}}_1(t) | \mathcal{U}(t), \boldsymbol{H}(t)) \tag{44}$$

$$\le \max_{\substack{\boldsymbol{C} \succeq 0, \\ \mathrm{tr}(\boldsymbol{C}) \le P}} \max_{\substack{p(\mathcal{U}(t)), \\ p(\boldsymbol{x}_2(t)|\mathcal{U}(t)) \\ \boldsymbol{K}(t) \preceq \boldsymbol{C}}} \left(\frac{1}{p} h(\bar{\boldsymbol{y}}_1(t), \bar{\boldsymbol{y}}_2(t) | \mathcal{U}(t), \boldsymbol{H}(t)) - \frac{1}{q} h(\bar{\boldsymbol{y}}_1(t) | \mathcal{U}(t), \boldsymbol{H}(t)) \right) \tag{45}$$

$$= \max_{\substack{\boldsymbol{C} \succeq 0, \\ \mathrm{tr}(\boldsymbol{C}) \le P}} \max_{\substack{p(\mathcal{U}(t)) \\ \boldsymbol{K}_u(t) \preceq \boldsymbol{C}}} \left(\frac{1}{p} h(\boldsymbol{S}(t)\boldsymbol{u}(t) + \boldsymbol{w}(t) | \mathcal{U}(t), \boldsymbol{H}(t)) - \frac{1}{q} h(\boldsymbol{H}_{12}(t)\boldsymbol{u}(t) + \boldsymbol{z}_1(t) | \mathcal{U}(t), \boldsymbol{H}(t)) \right) \tag{46}$$

$$= \max_{\substack{\boldsymbol{C} \succeq 0, \\ \mathrm{tr}(\boldsymbol{C}) \le P}} \max_{\substack{p(\hat{\boldsymbol{S}}(t)) \\ \boldsymbol{K}_u(t) \preceq \boldsymbol{C}}} \mathbb{E}_{\boldsymbol{S}(t), \hat{\boldsymbol{S}}(t)} \left(\frac{1}{p} \log\det(\mathbf{I} + \boldsymbol{S}(t)\boldsymbol{K}_u(t)\boldsymbol{S}^{\mathsf{H}}(t)) - \frac{1}{q} \log\det(\mathbf{I} + \boldsymbol{H}_{12}(t)\boldsymbol{K}_u(t)\boldsymbol{H}_{12}^{\mathsf{H}}(t)) \right) \tag{47}$$

$$\le \mathbb{E}_{\hat{\boldsymbol{S}}(t)} \max_{\substack{\boldsymbol{C} \succeq 0, \\ \mathrm{tr}(\boldsymbol{C}) \le P}} \max_{\substack{p(\hat{\boldsymbol{S}}(t)) \\ \boldsymbol{K}_u(t) \preceq \boldsymbol{C}}} \mathbb{E}_{\boldsymbol{S}(t) | \hat{\boldsymbol{S}}(t)} \left(\frac{1}{p} \log\det(\mathbf{I} + \boldsymbol{S}(t)\boldsymbol{K}_u(t)\boldsymbol{S}^{\mathsf{H}}(t)) - \frac{1}{q} \log\det(\mathbf{I} + \boldsymbol{H}_{12}(t)\boldsymbol{K}_u(t)\boldsymbol{H}_{12}^{\mathsf{H}}(t)) \right) \tag{48}$$

where (46) is obtained because Gaussian distributed vector $\boldsymbol{u}(t)$ maximizes the weighted difference of two differential entropies over all conditional distribution of $\boldsymbol{x}_2(t)$ with the same covariance matrix constraint, where $\boldsymbol{K}_u(t) \triangleq \mathbb{E}\{\boldsymbol{u}(t)\boldsymbol{u}^{\mathsf{H}}(t)\} = \max_{p(\mathcal{U}(t))} \boldsymbol{K}(t)$ when $p \ge q$ [16] and $\boldsymbol{w}(t) \triangleq [\boldsymbol{z}_1^{\mathsf{T}}(t)\ \boldsymbol{z}_2^{\mathsf{T}}(t)]^{\mathsf{T}}$; (47) is obtained because

(a) $\boldsymbol{u}(t)$ is Gaussian distributed with covariance matrix being relative to $(\boldsymbol{H}^{t-1}, \hat{\boldsymbol{H}}^{t})$ and hence independent of $\boldsymbol{S}(t)$ given $\hat{\boldsymbol{S}}(t)$ according to the assumption of Markov chain (4), (b) $\bar{\boldsymbol{y}}_1(t)$ is a degraded version of $(\bar{\boldsymbol{y}}_1(t), \bar{\boldsymbol{y}}_2(t))$; and (48) follows the fact that putting the expectation out of the maximization increases the value.

Letting $p = \min\{M, 2N\}$ and $q = \min\{M, N\}$, we have the following two cases:

1) Case $N < M < 2N$: Given $p = M$ and $q = N$, we have

$$\frac{1}{M} h(\bar{\boldsymbol{y}}_1(t), \bar{\boldsymbol{y}}_2(t)|\mathcal{U}(t), \boldsymbol{H}(t)) - \frac{1}{N} h(\bar{\boldsymbol{y}}_1(t)|\mathcal{U}(t), \boldsymbol{H}(t)) \tag{49}$$

$$\le \mathbb{E}_{\hat{\boldsymbol{S}}(t)} \max_{\substack{\boldsymbol{C}\succeq 0,\\ \mathrm{tr}(\boldsymbol{C})\le P}} \max_{\substack{p(\hat{\boldsymbol{S}}(t))\\ \boldsymbol{K}_u(t)\preceq \boldsymbol{C}}} \mathbb{E}_{\boldsymbol{S}(t)|\hat{\boldsymbol{S}}(t)} \frac{1}{MN} \left(N \log\det(\mathbf{I} + \boldsymbol{S}(t)\boldsymbol{K}_u(t)\boldsymbol{S}^{\mathsf{H}}(t)) - M \log\det(\mathbf{I} + \boldsymbol{H}_{12}(t)\boldsymbol{K}_u(t)\boldsymbol{H}_{12}^{\mathsf{H}}(t))\right) \tag{50}$$

$$\le \frac{M-N}{M} \alpha \log P + O(1) \tag{51}$$

where the last inequality is obtained from the following lemma:

Lemma 1. *For two random matrices $\boldsymbol{S} = \hat{\boldsymbol{S}} + \tilde{\boldsymbol{S}} \in \mathbb{C}^{2N\times M}$ and $\boldsymbol{H} = \hat{\boldsymbol{H}} + \tilde{\boldsymbol{H}} \in \mathbb{C}^{N\times M}$ $(N \le M \le 2N)$, where $\tilde{\boldsymbol{S}}$, $\tilde{\boldsymbol{H}}$ are respectively independent of $\hat{\boldsymbol{S}}$, $\hat{\boldsymbol{H}}$ and with each entry $\mathcal{N}_{\mathbb{C}}(0, \sigma^2)$ distributed, given any $\boldsymbol{K} \succeq 0$ with eigenvalues $\lambda_1 \ge \cdots \ge \lambda_M \ge 0$, we have*

$$N \mathbb{E}_{\tilde{\boldsymbol{S}}} \log\det(\mathbf{I} + \boldsymbol{S}\boldsymbol{K}\boldsymbol{S}^{\mathsf{H}}) - M \mathbb{E}_{\tilde{\boldsymbol{H}}} \log\det(\mathbf{I} + \boldsymbol{H}\boldsymbol{K}\boldsymbol{H}^{\mathsf{H}}) \le -N(M-N)\log(\sigma^2) + O(1) \tag{52}$$

as σ^2 goes to 0.

Proof: See Appendix B. ■

According to the Markov chain $\boldsymbol{X}_2^n \to \left(\bar{\boldsymbol{Y}}_1^n, \bar{\boldsymbol{Y}}_2^n\right) \to \bar{\boldsymbol{Y}}_1^n$, we upper-bound the weighted sum rate as

$$n\left(\frac{R_1}{N} + \frac{R_2}{M}\right) \tag{53}$$

$$\le n \log P + \sum_{t=1}^{n} \left(\frac{1}{M} h(\bar{\boldsymbol{y}}_1(t), \bar{\boldsymbol{y}}_2(t)|\mathcal{U}(t), \boldsymbol{H}(t)) - \frac{1}{N} h(\bar{\boldsymbol{y}}_1(t)|\mathcal{U}(t), \boldsymbol{H}(t))\right) + n\cdot O(1) + n\epsilon_n \tag{54}$$

$$\le n\left(1 + \frac{M-N}{M}\alpha\right)\log P + n\cdot O(1) + n\epsilon_n \tag{55}$$

and similarly obtain another outer bound by exchanging the roles of Rx-1 and Rx-2. Accordingly, the corresponding outer bounds of the DoF are obtained by the definition.

2) Case $M \ge 2N$: Given $p = 2N$ and $q = N$, we have

$$\frac{1}{2N} h(\bar{\boldsymbol{y}}_1(t), \bar{\boldsymbol{y}}_2(t)|\mathcal{U}(t), \boldsymbol{H}(t)) - \frac{1}{N} h(\bar{\boldsymbol{y}}_1(t)|\mathcal{U}(t), \boldsymbol{H}(t)) \tag{56}$$

$$\le \mathbb{E}_{\hat{\boldsymbol{S}}(t)} \max_{\substack{\boldsymbol{C}\succeq 0,\\ \mathrm{tr}(\boldsymbol{C})\le P}} \max_{\substack{p(\hat{\boldsymbol{S}}(t))\\ \boldsymbol{K}_u(t)\preceq \boldsymbol{C}}} \mathbb{E}_{\boldsymbol{S}(t)|\hat{\boldsymbol{S}}(t)} \frac{1}{2N} \left(\log\det(\mathbf{I} + \boldsymbol{H}_{22}(t)\boldsymbol{K}_u(t)\boldsymbol{H}_{22}^{\mathsf{H}}(t)) - \log\det(\mathbf{I} + \boldsymbol{H}_{12}(t)\boldsymbol{K}_u(t)\boldsymbol{H}_{12}^{\mathsf{H}}(t))\right) \tag{57}$$

$$\le \frac{1}{2}\alpha \log P + O(1) \tag{58}$$

where (57) follows from the inequality $\det(\mathbf{I} + \boldsymbol{A}) \le \det(\mathbf{I} + \boldsymbol{A}_{11})\det(\mathbf{I} + \boldsymbol{A}_{22})$ where $\boldsymbol{A}$ is an $2l \times 2l$ positive semidefinite matrix and $\boldsymbol{A}_{11}, \boldsymbol{A}_{22}$ are two $l \times l$ submatrices on the diagonal without overlap; and the last inequality follows the lemma:

Lemma 2. *For an* $N \times M$ *random matrix* ($M \geq N$) $\boldsymbol{H} = \hat{\boldsymbol{H}} + \tilde{\boldsymbol{H}}$ *where* $\tilde{\boldsymbol{H}}$ *with each entry* $\mathcal{N}_{\mathbb{C}}(0, \sigma^2)$ *distributed is independent of* $\hat{\boldsymbol{H}}$*, given any* $\boldsymbol{K} \succeq 0$ *with eigenvalues* $\lambda_1 \geq \cdots \geq \lambda_M \geq 0$*, we have the upper and lower bounds:*

$$\mathbb{E}_{\tilde{\boldsymbol{H}}} \log\det(\mathbf{I} + \boldsymbol{H}\boldsymbol{K}\boldsymbol{H}^{\mathsf{H}}) \leq \sum_{i=1}^{N} \log(1 + (\|\hat{\boldsymbol{H}}\|_F^2 + MN)\lambda_i) + O(1), \tag{59}$$

$$\mathbb{E}_{\tilde{\boldsymbol{H}}} \log\det(\mathbf{I} + \boldsymbol{H}\boldsymbol{K}\boldsymbol{H}^{\mathsf{H}}) \geq \sum_{i=1}^{N} \log(1 + \lambda_i \sigma^2 e^{\zeta}) + O(1). \tag{60}$$

The difference of the upper and lower bounds can be further bounded by

$$\log(1 + (\|\hat{\boldsymbol{H}}\|_F^2 + MN)\lambda_i) - \log(1 + \lambda_i \sigma^2 e^{\zeta}) \leq -\log(\sigma^2) + O(1) \tag{61}$$

where $\zeta \triangleq \frac{1}{N}\sum_{i=1}^{N} \psi(N-i+1)$ *and* $\psi(x)$ *is the digamma function that given by [17]* $\psi(x) = -\gamma + \sum_{p=1}^{x-1} \frac{1}{p} \leq \ln x + 1$ *for integer* x*, where* γ *is Euler's constant.*

Proof: See Appendix C. ■

In this case, the weighted sum rate can be bounded as

$$n(2R_1 + R_2) \tag{62}$$

$$\leq n \cdot 2N \log P + \sum_{t=1}^{n} \left(h(\bar{\boldsymbol{y}}_1(t), \bar{\boldsymbol{y}}_2(t) | \mathcal{U}(t), \boldsymbol{H}(t)) - 2h(\bar{\boldsymbol{y}}_1(t) | \mathcal{U}(t), \boldsymbol{H}(t))\right) + n \cdot O(1) + n\epsilon_n \tag{63}$$

$$\leq nN(2 + \alpha) \log P + n \cdot O(1) + n\epsilon_n \tag{64}$$

and another outer bound can be similarly obtained by exchanging the roles of Rx-1 and Rx-2. Accordingly, the corresponding outer bound of the DoF region is obtained by the definition.

V. ACHIEVABILITY

With delayed CSIT, MAT alignment employed in [3–6] takes into account the completely outdated CSIT, regardless of the correlation between current and previous channel states. In fact, however, the current CSI is predictable from the past states if the underlying channel exhibits some temporal correlation. By employing power allocation, superposition coding, and successive decoding techniques, recent results [10, 11, 13] demonstrated that the DoF region can be enlarged, where the benefit of the estimated current CSIT is fully exploitable even it is imperfect.

In the following, we extend such techniques to symmetric MIMO case, and construct a set of achievable schemes according to antenna configuration. In view of the similarity of achievable schemes of BC and IC, we only describe the corresponding schemes for IC avoiding redundancy. Three cases are considered:

- Case A: $M \leq N$
- Case B: $N < M < 2N$
- Case C: $M \geq 2N$

A. *Case A:* $M \leq N$

In this case, the DoF region with no CSIT coincides with that with perfect CSIT [7–9], indicating the delayed or current CSIT is of nothing benefit. In particular, all the DoF regions are achieved by simple time division and sharing.

B. *Case B:* $N < M < 2N$

To make the achievable schemes easily followable, we detail a particular setting with $M = 3$ and $N = 2$, where two vertices

$$P_{B1}:\ (2, \alpha), \quad P_{B2}:\ \left(\frac{6+4\alpha}{5}, \frac{6-\alpha}{5}\right) \tag{65}$$

are achievable as shown in Fig. 2. We relegate the generalized version to the Appendix D.

Before proceeding further, we define

$$\boldsymbol{Q}_{ij}(t) \in \mathbb{C}^{3\times 2} \subseteq \mathcal{R}\{\hat{\boldsymbol{H}}_{ij}(t)\}, \qquad \boldsymbol{Q}_{ij}^{\perp}(t) \in \mathbb{C}^{3\times 1} \subseteq \mathcal{N}\{\hat{\boldsymbol{H}}_{ij}(t)\}, \tag{66a}$$

$$\boldsymbol{W}(t) \in \mathbb{C}^{3\times 1} \subseteq \mathcal{R}\{\hat{\boldsymbol{H}}_{211}(t)\}, \qquad \boldsymbol{W}^{\perp}(t) \in \mathbb{C}^{3\times 2} \subseteq \mathcal{N}\{\hat{\boldsymbol{H}}_{211}(t)\}, \tag{66b}$$

where $\hat{\boldsymbol{H}}_{211}(t)$ is the first row of $\hat{\boldsymbol{H}}_{21}(t)$. Note that the range and null spaces represent column space for notational conciseness. Note also that $\boldsymbol{W}(t)$ and $\boldsymbol{W}^{\perp}(t)$ lie in the range and null spaces of the first row of $\hat{\boldsymbol{H}}_{21}(t)$, respectively. According to the definition of imperfect current CSIT, we have $\mathbb{E}\|\boldsymbol{H}_{ji}(t)\boldsymbol{Q}_{ji}^{\perp}(t)\|_{\mathrm{F}}^2 \sim P^{-\alpha}$ and $\mathbb{E}\|\boldsymbol{H}_{211}(t)\boldsymbol{W}^{\perp}(t)\|_{\mathrm{F}}^2 \sim P^{-\alpha}$.

Achievability of $P_{B1}: (2, \alpha)$

This vertex can be achieved within one single slot (we drop time index here for conciseness) by transmitting codewords with superposition coding [19] as

$$\boldsymbol{x}_1 = \boldsymbol{Q}_{11}\boldsymbol{u}_c + \boldsymbol{W}^{\perp}\boldsymbol{u}_p, \quad \boldsymbol{x}_2 = \boldsymbol{Q}_{12}^{\perp} v_p \tag{67}$$

where $\boldsymbol{u}_c \in \mathbb{C}^{2\times 1}$ with each symbol of rate $(1-\alpha)\log P$ is decodable by both receivers (referred to as *common message*) but only desirable by Rx-1, and $\boldsymbol{u}_p \in \mathbb{C}^{2\times 1}$, v_p with each element of rate $\alpha \log P$ can only be seen by its respective receiver (referred to as *private messages*), satisfying power constraints $\mathbb{E}\|\boldsymbol{u}_c\|^2 \leq P$ and $\mathbb{E}\|\boldsymbol{u}_p\|^2 = \mathbb{E}|v_p|^2 \leq P^{\alpha}$. At the receiver side, we have (with noise terms being omitted hereafter for conciseness)

$$\boldsymbol{y}_1 = \underbrace{\boldsymbol{H}_{11}\boldsymbol{Q}_{11}\boldsymbol{u}_c}_{P} + \underbrace{\boldsymbol{H}_{11}\boldsymbol{W}^{\perp}\boldsymbol{u}_p}_{P^{\alpha}} + \underbrace{\boldsymbol{H}_{12}\boldsymbol{Q}_{12}^{\perp}v_p}_{P^0}, \tag{68a}$$

$$\boldsymbol{y}_2 = \underbrace{\boldsymbol{H}_{21}\boldsymbol{Q}_{11}\boldsymbol{u}_c}_{P} + \underbrace{\boldsymbol{H}_{21}\boldsymbol{W}^{\perp}\boldsymbol{u}_p + \boldsymbol{H}_{22}\boldsymbol{Q}_{12}^{\perp}v_p}_{P^{\alpha}}, \tag{68b}$$

$$y_{21} = \underbrace{\boldsymbol{H}_{211}\boldsymbol{Q}_{11}\boldsymbol{u}_c}_{P} + \underbrace{\boldsymbol{H}_{211}\boldsymbol{W}^{\perp}\boldsymbol{u}_p}_{P^0} + \underbrace{\boldsymbol{H}_{212}\boldsymbol{Q}_{12}^{\perp}v_p}_{P^{\alpha}}, \tag{68c}$$

where y_{21} is the first element of $\boldsymbol{y}_2$. The common (cf. $\boldsymbol{u}_c$) and private (cf. $\boldsymbol{u}_p$ and v_p) messages are recoverable by successive decoding [19], which takes three steps: (i) retrieving 2×1 vector $\boldsymbol{u}_c$ first with *all* receive antennas by treating others as noise, from 2 linearly independent equations each [cf. (68a)-(68b)], yielding in total $2(1-\alpha)$ DoF desired only by Rx-1; (ii) reconstructing the whole terms $\boldsymbol{H}_{11}\boldsymbol{Q}_{11}\boldsymbol{u}_c$ in (68a) and $\boldsymbol{H}_{211}\boldsymbol{Q}_{11}\boldsymbol{u}_c$ in (68c), and consequently subtracting them from received signals; (iii) recovering the private messages $\boldsymbol{u}_p$ (resp. v_p) from the residual signal in (68a) at the Rx-1 [resp. in (68c) at the Rx-2], yielding 2α DoF for Rx-1 (resp. α DoF for Rx-2). We point out that, in the last two steps only the signal at the *first* antenna of Rx-2 is considered [cf. y_{21}], where the interference arisen from $\boldsymbol{u}_p$ is pre-canceled by precoder $\boldsymbol{W}^{\perp}$. It is worth noting that the numbers of private messages for both receivers are imbalanced due to the limited dimensionalities, i.e., $M \leq 2N$.

In the end, Rx-1 achieves the total 2 DoF while Rx-2 obtains α DoF. By exchanging the roles of the two receivers, the DoF pair $(\alpha, 2)$ can be achieved in a similar way.

Achivability of $P_{B2} : \left(\frac{6+4\alpha}{5}, \frac{6-\alpha}{5}\right)$

Similarly to the case with pure delayed CSIT [5, 6], $(M+N)=5$ time slots are required to achieve such point, but in a much more involved way. In the following, we first provide a variant of MAT alignment, followed by a new scheme integrating the imperfect current CSIT.

1) A Variant of MAT Alignment: With $M=3$ and $N=2$, the original MAT alignment for MIMO IC can be achieved in a different fashion with two phases: data symbols are sent all together in the first phase whereas the overheard interferences are forwarded in the second phase, as illustrated in Fig. 3.

Phase-1 ($N=2$ slots): The transmitted signals can be given by

$$\boldsymbol{x}_1(t) = \boldsymbol{u}(t), \quad \boldsymbol{x}_2(t) = \boldsymbol{v}(t), \quad t = 1, 2 \tag{69}$$

where $\boldsymbol{u}(t), \boldsymbol{v}(t) \in \mathbb{C}^{3\times 1}$. The received signals of $N=2$ antennas at the RX-1 and the first $M-N=1$ antenna at the Rx-2, where in total $M=3$ receive antennas are sufficient, are given by

$$\boldsymbol{y}_1(t) = \boldsymbol{H}_{11}(t)\boldsymbol{x}_1(t) + \underbrace{\boldsymbol{H}_{12}(t)\boldsymbol{x}_2(t)}_{\boldsymbol{\eta}_t^1}, \tag{70a}$$

$$y_{21}(t) = \underbrace{\boldsymbol{H}_{211}(t)\boldsymbol{x}_1(t)}_{\eta_{t1}^2} + \boldsymbol{H}_{212}(t)\boldsymbol{x}_2(t), \tag{70b}$$

where $\boldsymbol{\eta}_t^1 = [\eta_{t1}^1 \; \eta_{t2}^1]^{\mathsf{T}}$. Note that after two slots the Rx-1 requires $\{\eta_{tk}^1, t, k = 1, 2\}$ to cancel the interferences as well as another $M-N=1$ linearly independent equation which can be obtained by $\{\eta_{t1}^2, t=1,2\}$ to retrieve $\boldsymbol{u}(t)$. On the other hand, the Rx-2 requires $\{\eta_{t1}^2, t=1,2\}$ to cancel the interferences at the first $(M-N=1)$ antenna as well as another $N=2$ linearly independent equations provided by $\{\eta_{tk}^1, t, k=1,2\}$ to retrieve $\boldsymbol{v}(t)$. After Phase-1, the transmitter has access to $\boldsymbol{H}_{ij}(t)$ $(t=1,2)$. Together with the transmitted symbols, it can reconstruct the total $MN=6$ interference terms $\eta_{11}^1, \eta_{12}^1, \eta_{21}^1, \eta_{22}^1, \eta_{11}^2, \eta_{21}^2$. All of them will be delivered in the following $M=3$ time slots, where in each slot $N=2$ terms are sent.

Phase-2 ($M=3$ slots): Before forwarding the interference terms, we concatenate them into $M=3$ vectors, e.g., $\bar{\boldsymbol{\eta}}_1^1 \triangleq [\eta_{11}^1 \, \eta_{21}^1]^{\mathsf{T}}$, $\bar{\boldsymbol{\eta}}_2^1 \triangleq [\eta_{12}^1 \, \eta_{22}^1]^{\mathsf{T}}$ and $\bar{\boldsymbol{\eta}}_1^2 \triangleq [\eta_{11}^2 \, \eta_{21}^2]^{\mathsf{T}}$. With such interference grouping, we construct the transmitted signal as

$$\begin{cases} \boldsymbol{x}_1(3) = 0 \\ \boldsymbol{x}_2(3) = \boldsymbol{\Phi}(3)\bar{\boldsymbol{\eta}}_1^1 \end{cases}, \begin{cases} \boldsymbol{x}_1(4) = 0 \\ \boldsymbol{x}_2(4) = \boldsymbol{\Phi}(4)\bar{\boldsymbol{\eta}}_2^1 \end{cases}, \begin{cases} \boldsymbol{x}_1(5) = \boldsymbol{\Phi}(5)\bar{\boldsymbol{\eta}}_1^2 \\ \boldsymbol{x}_2(5) = 0 \end{cases} \tag{71}$$

where $\boldsymbol{\Phi}(t) \in \mathbb{C}^{3\times 2}$ $(t = 3, 4, 5)$ are random matrices, as shown in Fig. 3. With $N = 2$ antennas at each receiver, $\bar{\boldsymbol{\eta}}_k^i$ $(i = 1, 2)$ can be successfully recovered. As stated above, with the required interference terms as well as sufficient linearly independent equations, the transmitted symbols in Phase-1 are all recoverable, yielding $\frac{MN}{M+N} = \frac{6}{5}$ DoF for each Tx-Rx pair.

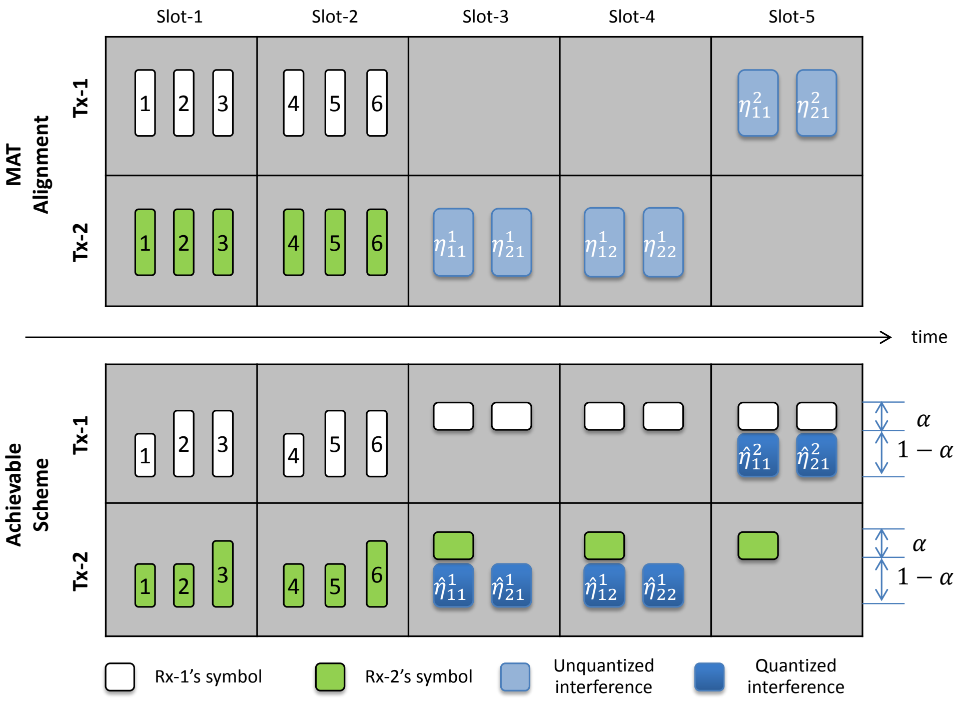

Fig. 3: Illustration of the difference between MAT alignment and the achievable scheme for $(3, 2)$ MIMO IC, where the height of the brick indicates the data rate in terms of $\log P$.

2) Integrating Imperfect Current CSIT: With the imperfect current CSIT, the new transmission scheme follows a similar step to the aforementioned MAT variant, but together with the philosophy developed in [10, 11]:

- Precoding and proper power allocation: Instead of sending the crude symbols like in (69), we now exploit the spatial precoding to send two symbols to each user as

$$\begin{aligned} \boldsymbol{x}_1(t) &= \begin{bmatrix} \boldsymbol{W}(t) & \boldsymbol{W}^{\perp}(t) \end{bmatrix} \boldsymbol{u}(t), \\ \boldsymbol{x}_2(t) &= \begin{bmatrix} \boldsymbol{Q}_{12}(t) & \boldsymbol{Q}_{12}^{\perp}(t) \end{bmatrix} \boldsymbol{v}(t), \end{aligned} \quad t = 1, 2 \tag{72}$$

  and assign $P^{1-\alpha}$, P, P to three symbols in $\boldsymbol{u}(t)$ whereas $P^{1-\alpha}$, $P^{1-\alpha}$, P to three symbols in $\boldsymbol{v}(t)$, as shown in the first two blocks of Fig. 3. It follows that the effective rates of $\boldsymbol{u}(t)$ and $\boldsymbol{v}(t)$ in each slot are

$(3-\alpha)\log P$ and $(3-2\alpha)\log P$, respectively. It therefore generates $MN=6$ interferences in total, i.e.,

$$\begin{aligned} \boldsymbol{\eta}_t^1 &= \boldsymbol{H}_{12}(t)\begin{bmatrix}\boldsymbol{Q}_{12}(t) & \boldsymbol{Q}_{12}^{\perp}(t)\end{bmatrix}\boldsymbol{v}(t), \\ \eta_{t1}^2 &= \boldsymbol{H}_{211}(t)\begin{bmatrix}\boldsymbol{W}(t) & \boldsymbol{W}^{\perp}(t)\end{bmatrix}\boldsymbol{u}(t), \end{aligned} \quad t=1,2 \tag{73}$$

where $\boldsymbol{Q}_{12}(t)\in\mathbb{C}^{3\times 2}$, $\boldsymbol{Q}_{12}^{\perp}(t)\in\mathbb{C}^{3\times 1}$, $\boldsymbol{W}(t)\in\mathbb{C}^{3\times 1}$, $\boldsymbol{W}^{\perp}(t)\in\mathbb{C}^{3\times 2}$, $\boldsymbol{\eta}_t^1\in\mathbb{C}^{2\times 1}$ and η_{t1}^2 is a scalar. Recalling the property of the precoders in (66), we know that the interference terms $\boldsymbol{\eta}_k^1$ and η_{k1}^2 in Phase-1 have a power scaling as $P^{1-\alpha}$. As did in the previous subsection, we pack these interferences into $M=3$ vectors: $\bar{\boldsymbol{\eta}}_1^1=[\eta_{11}^1\ \eta_{21}^1]^{\intercal}$, $\bar{\boldsymbol{\eta}}_2^2=[\eta_{12}^1\ \eta_{22}^1]^{\intercal}$, and $\bar{\boldsymbol{\eta}}_1^2=[\eta_{11}^2\ \eta_{21}^2]^{\intercal}$.

- Quantization and digital retransmission: Instead of forwarding $\bar{\boldsymbol{\eta}}_k^i$ $(i=1,2)$ directly, we quantize them with source codebook size of $(1-\alpha)\log P$ bits each, which makes the quantization error negligible in terms of DoF, and then retransmit their indices, denoted by $\hat{\boldsymbol{\eta}}_k^i$ $(i=1,2)$, in a digital fashion. The feasibility of such digital transmission is demonstrated in details in [11].
- Superposition coding and successive decoding: On top of codewords of the digitalized interferences $\hat{\boldsymbol{\eta}}_k^i$ $(i=1,2)$ with each element of rate $(1-\alpha)\log P$ (cf. common message), we encode another fresh symbols (cf. private message) with rate $\alpha\log P$ each by using superposition coding techniques [19], i.e.,

$$\begin{cases} \boldsymbol{x}_1(3)=\boldsymbol{W}^{\perp}(3)\boldsymbol{u}_p(1) \\ \boldsymbol{x}_2(3)=\boldsymbol{\Phi}(3)\hat{\boldsymbol{\eta}}_1^1+\boldsymbol{Q}_{12}^{\perp}(3)v_p(1) \end{cases}, \begin{cases} \boldsymbol{x}_1(4)=\boldsymbol{W}^{\perp}(4)\boldsymbol{u}_p(2) \\ \boldsymbol{x}_2(4)=\boldsymbol{\Phi}(4)\hat{\boldsymbol{\eta}}_2^1+\boldsymbol{Q}_{12}^{\perp}(4)v_p(2) \end{cases}, \begin{cases} \boldsymbol{x}_1(5)=\boldsymbol{\Phi}(5)\hat{\boldsymbol{\eta}}_1^2+\boldsymbol{W}^{\perp}(3)\boldsymbol{u}_p(3) \\ \boldsymbol{x}_2(5)=\boldsymbol{Q}_{12}^{\perp}(5)v_p(3) \end{cases}$$

where $\boldsymbol{u}_p(s)\in\mathbb{C}^{2\times 1},\ s=1,2,3$ and $v_p(s)$ is a scalar. Note that the power allocation satisfies $\mathbb{E}\|\hat{\boldsymbol{\eta}}_k^i\|^2\le P$ whereas $\mathbb{E}\|\boldsymbol{u}_p(s)\|^2\le P^{\alpha}$ and $\mathbb{E}|v_p(s)|^2\le P^{\alpha}$. Thus, the received signal in Slot-3 can be given by (those in other slots can be similarly obtained)

$$\boldsymbol{y}_1(3)=\underbrace{\boldsymbol{H}_{12}(3)\boldsymbol{\Phi}(3)\hat{\boldsymbol{\eta}}_1^1}_{P}+\underbrace{\boldsymbol{H}_{11}(3)\boldsymbol{W}^{\perp}(3)\boldsymbol{u}_p(1)}_{P^{\alpha}}+\underbrace{\boldsymbol{H}_{12}(3)\boldsymbol{Q}_{12}^{\perp}(3)v_p(1)}_{P^0}, \tag{74a}$$

$$\boldsymbol{y}_2(3)=\underbrace{\boldsymbol{H}_{22}(3)\boldsymbol{\Phi}(3)\hat{\boldsymbol{\eta}}_1^1}_{P}+\underbrace{\boldsymbol{H}_{21}(3)\boldsymbol{W}^{\perp}(3)\boldsymbol{u}_p(1)+\boldsymbol{H}_{22}(3)\boldsymbol{Q}_{12}^{\perp}(3)v_p(1)}_{P^{\alpha}}, \tag{74b}$$

$$y_{21}(3)=\underbrace{\boldsymbol{H}_{212}(3)\boldsymbol{\Phi}(3)\hat{\boldsymbol{\eta}}_1^1}_{P}+\underbrace{\boldsymbol{H}_{211}(3)\boldsymbol{W}^{\perp}(3)\boldsymbol{u}_p(1)}_{P^0}+\underbrace{\boldsymbol{H}_{212}(3)\boldsymbol{Q}_{12}^{\perp}(3)v_p(1)}_{P^{\alpha}}. \tag{74c}$$

At the receivers, by successive decoding described in the previous subsection, both the common (cf. $\hat{\boldsymbol{\eta}}_1^1$) and private [cf. $\boldsymbol{u}_p(1)$ for Rx-1 and $v_p(1)$ for Rx-2] messages can be successively decoded, yielding 2α (resp. α) DoF from private messages $\boldsymbol{u}_p(1)$ for Rx-1 [resp. $v_p(1)$ for Rx-2]. Those for Slot-4 and Slot-5 can be similarly deduced. In the end, the codeword vector $\hat{\boldsymbol{\eta}}_1^1$, $\hat{\boldsymbol{\eta}}_2^1$ and $\hat{\boldsymbol{\eta}}_1^2$ can be all recovered (and in turn $\boldsymbol{\eta}_k^1$ and η_{k1}^1 with negligible quantization error) at both receivers, serving to cancel the overheard interference as well as to provide additional linearly independent equations for $\boldsymbol{u}(t)$ and $\boldsymbol{v}(t)$, $t=1,2$. Both with $MN=6$ linearly independent equations, the vectors $\boldsymbol{u}(t)$ and $\boldsymbol{v}(t)$ $(t=1,2)$ with total $MN=6$ symbols each are recoverable at its respective receiver. As illustrated in Fig. 3, the DoF pair $\left(\frac{6+4\alpha}{5},\frac{6-\alpha}{5}\right)$ is therefore achieved.

C. Case C: $M \geq 2N$

Due to the fact that additional transmit antennas do not increase DoF as long as $M \geq 2N$ in both perfect instantaneous and delayed CSIT setting [2, 5], we consider $M = 2N$ case here for illustration. With for instance $M = 4$ and $N = 2$, we demonstrate the outer bound in Theorem 1 is tight (as Theorem 2 claimed), where the vertices

$$P_{C1}: \ (2, 2\alpha), \quad P_{C2}: \ \left(\frac{4+2\alpha}{3}, \frac{4+2\alpha}{3}\right) \tag{75}$$

and their counterparts (with exchanged roles of both receivers) are all achievable as shown in Fig. 1. Note that this case coincides with the MISO case except for the multiplication factor of 2. We therefore relegate the generalization to the Appendix E.

Following the similar definition, we have

$$\boldsymbol{Q}_{ij}(t) \in \mathbb{C}^{4\times 2} \subseteq \mathcal{R}\{\hat{\boldsymbol{H}}_{ij}(t)\}, \qquad \boldsymbol{Q}_{ij}^{\perp}(t) \in \mathbb{C}^{4\times 2} \subseteq \mathcal{N}\{\hat{\boldsymbol{H}}_{ij}(t)\} \tag{76}$$

where $\mathbb{E}\|\boldsymbol{H}_{ji}(t)\boldsymbol{Q}_{ji}^{\perp}(t)\|_{\mathrm{F}}^2 \sim P^{-\alpha}$.

Achievability of $P_{C1}: (2, 2\alpha)$

This vertex can be achieved within one single slot. The transmission with superposition coding can be given by

$$\boldsymbol{x}_1 = \boldsymbol{Q}_{11}\boldsymbol{u}_c + \boldsymbol{Q}_{21}^{\perp}\boldsymbol{u}_p, \quad \boldsymbol{x}_2 = \boldsymbol{Q}_{12}^{\perp}\boldsymbol{v}_p \tag{77}$$

where $\boldsymbol{u}_c \in \mathbb{C}^{2\times 1}$ is a common message and decodable by both receivers but only desirable by Rx-1, and $\boldsymbol{u}_p, \ \boldsymbol{v}_p \in \mathbb{C}^{2\times 1}$ are private messages which can only be seen and decoded by their corresponding receivers. These transmitted symbols are assumed to satisfy the power constraints $\mathbb{E}\|\boldsymbol{u}_c\|^2 \leq P$ with each symbol of rate $(1-\alpha)\log P$, and $\mathbb{E}\|\boldsymbol{u}_p\|^2 = \mathbb{E}\|\boldsymbol{v}_p\|^2 \leq P^{\alpha}$ with each symbol of rate $\alpha \log P$. At the receiver side, we have

$$\boldsymbol{y}_1 = \underbrace{\boldsymbol{H}_{11}\boldsymbol{Q}_{11}\boldsymbol{u}_c}_{P} + \underbrace{\boldsymbol{H}_{11}\boldsymbol{Q}_{21}^{\perp}\boldsymbol{u}_p}_{P^{\alpha}} + \underbrace{\boldsymbol{H}_{12}\boldsymbol{Q}_{12}^{\perp}\boldsymbol{v}_p}_{P^0}, \tag{78a}$$

$$\boldsymbol{y}_2 = \underbrace{\boldsymbol{H}_{21}\boldsymbol{Q}_{11}\boldsymbol{u}_c}_{P} + \underbrace{\boldsymbol{H}_{21}\boldsymbol{Q}_{21}^{\perp}\boldsymbol{u}_p}_{P^0} + \underbrace{\boldsymbol{H}_{22}\boldsymbol{Q}_{12}^{\perp}\boldsymbol{v}_p}_{P^{\alpha}}. \tag{78b}$$

By successive decoding, both the common (cf. $\boldsymbol{u}_c$) and private (cf. $\boldsymbol{u}_p, \ \boldsymbol{v}_p$) messages can be subsequently decoded, yielding total 2 and 2α DoF for Rx-1 and Rx-2, respectively.

Achievability of $P_{C2}: \left(\frac{4+2\alpha}{3}, \frac{4+2\alpha}{3}\right)$

Differently from the Case B, three time slots are sufficient to achieve such a vertex, which can be straightforwardly extended from the MISO case [13].

Slot-1: The transmitted signals from both transmitters are given by

$$\boldsymbol{x}_1(1) = \begin{bmatrix}\boldsymbol{Q}_{21}(1) & \boldsymbol{Q}_{21}^{\perp}(1)\end{bmatrix}\boldsymbol{u}(1), \tag{79a}$$

$$\boldsymbol{x}_2(1) = \begin{bmatrix}\boldsymbol{Q}_{12}(1) & \boldsymbol{Q}_{12}^{\perp}(1)\end{bmatrix}\boldsymbol{v}(1), \tag{79b}$$

where $\boldsymbol{u}(1) \triangleq [\boldsymbol{u}_1^{\mathsf{T}}(1)\ \boldsymbol{u}_2^{\mathsf{T}}(1)]^{\mathsf{T}}$, $\boldsymbol{v}(1) \triangleq [\boldsymbol{v}_1^{\mathsf{T}}(1)\ \boldsymbol{v}_2^{\mathsf{T}}(1)]^{\mathsf{T}}$ with $\boldsymbol{u}_i(1), \boldsymbol{v}_i(1) \in \mathbb{C}^{2\times 1}$. At both receivers, we have

$$\boldsymbol{y}_1(1) = \boldsymbol{H}_{11}(1)\begin{bmatrix}\boldsymbol{Q}_{21}(1) & \boldsymbol{Q}_{21}^{\perp}(1)\end{bmatrix}\boldsymbol{u}(1) + \underbrace{\boldsymbol{H}_{12}(1)\begin{bmatrix}\boldsymbol{Q}_{12}(1) & \boldsymbol{Q}_{12}^{\perp}(1)\end{bmatrix}\boldsymbol{v}(1)}_{\boldsymbol{\eta}_1}, \tag{80a}$$

$$\boldsymbol{y}_2(1) = \underbrace{\boldsymbol{H}_{21}(1)\begin{bmatrix}\boldsymbol{Q}_{21}(1) & \boldsymbol{Q}_{21}^{\perp}(1)\end{bmatrix}\boldsymbol{u}(1)}_{\boldsymbol{\eta}_2} + \boldsymbol{H}_{22}(1)\begin{bmatrix}\boldsymbol{Q}_{12}(1) & \boldsymbol{Q}_{12}^{\perp}(1)\end{bmatrix}\boldsymbol{v}(1), \tag{80b}$$

where $\boldsymbol{\eta}^i \in \mathbb{C}^{2\times 1},\ i = 1, 2$. By balancing the allocated power among those vectors, i.e., $\mathbb{E}\|\boldsymbol{u}_1(1)\|^2 = \mathbb{E}\|\boldsymbol{v}_1(1)\|^2 \sim P^{1-\alpha}$ and $\mathbb{E}\|\boldsymbol{u}_2(1)\|^2 = \mathbb{E}\|\boldsymbol{v}_2(1)\|^2 = P - 2P^{1-\alpha} \sim P$, we approximate the total power of interference as $\mathbb{E}\|\boldsymbol{\eta}_1\|^2 \sim P^{1-\alpha}$ and $\mathbb{E}\|\boldsymbol{\eta}_2\|^2 \sim P^{1-\alpha}$. Accordingly, the effective transmission rate of Slot-1 is $(4-2\alpha)\log P$ for each Tx-Rx pair. As did in the previous section, the interferences are first quantized and then retransmitted in the digital fashion. Denoted by $\hat{\boldsymbol{\eta}}_i$ $(i = 1, 2)$ the indices of the quantized version, the digitalized interference are forwarded in the ensuing two slots.

Slot-2 & Slot-3: These two slots are similar. In Slot-2 (resp. Slot-3), apart from the forwarding of the digitalized interferences $\hat{\boldsymbol{\eta}}_2$ (resp. $\hat{\boldsymbol{\eta}}_1$), the Tx-1 (resp. Tx-2) sends a new symbol vector with superposition coding, while only a new symbol vector at the Tx-2 (resp. Tx-1). The transmitted signals in two slots are

$$\text{Slot-2:}\quad \begin{aligned}\boldsymbol{x}_1(2) &= \boldsymbol{Q}_{21}(2)\hat{\boldsymbol{\eta}}_2 + \boldsymbol{Q}_{21}^{\perp}(2)\boldsymbol{u}(2)\\ \boldsymbol{x}_2(2) &= \boldsymbol{Q}_{12}^{\perp}(2)\boldsymbol{v}(2)\end{aligned} \tag{81a}$$

$$\text{Slot-3:}\quad \begin{aligned}\boldsymbol{x}_1(3) &= \boldsymbol{Q}_{21}^{\perp}(3)\boldsymbol{u}(3)\\ \boldsymbol{x}_2(3) &= \boldsymbol{Q}_{12}(3)\hat{\boldsymbol{\eta}}_1 + \boldsymbol{Q}_{12}^{\perp}(3)\boldsymbol{v}(3)\end{aligned} \tag{81b}$$

where $\hat{\boldsymbol{\eta}}_i \in \mathbb{C}^{2\times 1},\ i = 1, 2$ are treated as common messages with each element of rate $(1-\alpha)\log P$ and power constraint $\mathbb{E}\|\hat{\boldsymbol{\eta}}_i\|^2 \le P$, and $\boldsymbol{u}(2), \boldsymbol{v}(2), \boldsymbol{u}(3), \boldsymbol{v}(3) \in \mathbb{C}^{2\times 1}$ are private messages with each symbol of rate $\alpha \log P$, satisfying $\mathbb{E}\|\boldsymbol{u}(t)\|^2 = \mathbb{E}\|\boldsymbol{v}(t)\|^2 \le P^{\alpha}$, $t = 2, 3$.

In Slot-2, the received signals are give by (the received signals in Slot-3 can be similarly obtained)

$$\boldsymbol{y}_1(2) = \underbrace{\boldsymbol{H}_{11}(2)\boldsymbol{Q}_{21}(2)\hat{\boldsymbol{\eta}}_2}_{P} + \underbrace{\boldsymbol{H}_{11}(2)\boldsymbol{Q}_{21}^{\perp}(2)\boldsymbol{u}(2)}_{P^{\alpha}} + \underbrace{\boldsymbol{H}_{12}(2)\boldsymbol{Q}_{12}^{\perp}(2)\boldsymbol{v}(2)}_{P^{0}}, \tag{82a}$$

$$\boldsymbol{y}_2(2) = \underbrace{\boldsymbol{H}_{21}(2)\boldsymbol{Q}_{21}(2)\hat{\boldsymbol{\eta}}_2}_{P} + \underbrace{\boldsymbol{H}_{21}(2)\boldsymbol{Q}_{21}^{\perp}(2)\boldsymbol{u}(2)}_{P^{0}} + \underbrace{\boldsymbol{H}_{22}(2)\boldsymbol{Q}_{12}^{\perp}(2)\boldsymbol{v}(2)}_{P^{\alpha}}. \tag{82b}$$

By successive decoding described in the previous subsection, both the common message (cf. $\hat{\boldsymbol{\eta}}_2$) and the private messages [cf. $\boldsymbol{u}(2)$ for Rx-1 and $\boldsymbol{v}(2)$ for RX-2] are retrievable provided 2 linearly independent equations at their respective receivers. The same strategy applies to Slot-3.

In the end, 2×1 codeword vector $\hat{\boldsymbol{\eta}}_2$ and $\hat{\boldsymbol{\eta}}_1$ can be all recovered (and in turn $\boldsymbol{\eta}_1$ and $\boldsymbol{\eta}_2$ with negligible quantization error) at both receivers, serving to cancel the overheard interference as well as to provide additional linearly independent equations for $\boldsymbol{v}(1)$ and $\boldsymbol{u}(1)$, respectively. With 4 linearly independent equations, the 4×1 vectors $\boldsymbol{u}(1)$ and $\boldsymbol{v}(1)$ are both recoverable with high probability at their respective receivers. Hence, the total $(4 + 2\alpha)$ DoF for each receiver is achieved within three time slots, and in turn P_{C2} is achievable by symmetry.

VI. CONCLUSION

In this work, we focus on the two-user MIMO broadcast and interference channels where the transmitter(s) has/have access to both delayed CSIT and an estimate of current CSIT. Specifically, the DoF region of one important MIMO scenario offered by the same numbers of transmit and receive antennas is characterized, relying on the forwarding to users of a suitably quantized version of prior interference obtained under imperfect linear ZF precoding at the transmitter(s). With multiple antennas at the receiver, the additional spatial dimension enables to cancel a certain amount of residual interference generated by the impreciseness of transmit precoding, and thus further enhances the achievable DoF. Our DoF region covers a family of CSIT settings, coinciding with previously reported results for extreme situations such as pure delayed CSIT and pure current CSIT. The extension to the more general MIMO cases with arbitrary number of antennas is still an open and challenging problem.

APPENDIX

A. Preliminaries

Before proceeding further, we provide the following preliminary results.

Let $\boldsymbol{A} \in \mathbb{C}^{N \times M}$, $N \le M$, be a full rank matrix and $\boldsymbol{A}' \in \mathbb{C}^{N \times M'}$, $M' \le M$, be a submatrix of $\boldsymbol{A}$. We have the following lemmas that will be repeatedly used in the rest of the proof.

Lemma 3 (rank of submatrix)**.**

$$\operatorname{rank}(\boldsymbol{A}') \ge \operatorname{rank}(\boldsymbol{A}) - (M - M'). \tag{83}$$

Lemma 4. *Let* $\mathcal{I}_1, \dots, \mathcal{I}_M$ *be a cyclic sliding window of size* N *on the set of indices* $\{1, \dots, M\}$*, i.e.,*

$$\mathcal{I}_k \triangleq \{(k+i)_M + 1 \, : i \in [0, N-1]\}, \quad k = 1, \dots, M. \tag{84}$$

If the columns of $\boldsymbol{A}$ *are arranged such that* $\operatorname{rank}(\boldsymbol{A}_{\mathcal{I}_k}) = N$ *for some* $k \in [1, M]$*, then*

$$\sum_{k=1}^{M} \operatorname{rank}(\boldsymbol{A}_{\mathcal{I}_k}) \ge N^2 \tag{85}$$

where $\boldsymbol{A}_{\mathcal{I}_k}$ *is the matrix composed of* N *columns of* $\boldsymbol{A}$ *defined by* $\mathcal{I}_k$*, i.e.,* $\boldsymbol{A}_{\mathcal{I}_k} \triangleq [A_{j,i}]_{j \in [1,N], i \in \mathcal{I}_k}$.

Proof: The sketch of the proofs for the above lemma is illustrated in Fig. 4(a). Given that there exists k such that the submatrix selected by the window is full rank N (the blue window in Fig.4(a)), the rank of the submatrix selected by the window $\mathcal{I}_{k+1}$ or $\mathcal{I}_{k-1}$ (the red window in Fig.4(b)) is lower bounded by $N-1$. By applying the same argument, it is readily shown that the rank of the submatrix selected by the window $\mathcal{I}_{k+2}$ or $\mathcal{I}_{k-2}$ is lower bounded by $N-2$. This lower bound keeps decreasing when the window slides away from the blue one, until it hits another lower bound $N-(M-N)=2N-M$ given by Lemma 3. The submatrices within the sliding windows are of rank $2N-M$, which lasts $M-1-2(M-N)=2N-M-1$ times. With the help of Fig.4(a), a lower bound on the sum of the ranks of all the submatrices visited by the sliding window, can be obtained by counting the dots in the Figure, i.e.,

$$N+2\sum_{i=1}^{M-N}(N-i)+(2N-M)(2N-M+1)=N^2. \tag{86}$$

In fact, this can be found easily by "completing the triangle", the number of dots in which is N^2. ■

Lemma 5. *$\boldsymbol{A}' \in \mathbb{C}^{N\times M'}$, $N \le M' \le M$, is a submatrix of $\boldsymbol{A}$. We define $\mathcal{I}'_1,\dots,\mathcal{I}'_{M'}$ as a cyclic sliding window of size N on the set of indices $\{1,\dots,M'\}$, i.e.,*

$$\mathcal{I}'_k \triangleq \{(k+i)_{M'}+1\ : i\in[0,N-1]\},\quad k=1,\dots,M'. \tag{87}$$

If the columns of $\boldsymbol{A}'$ are arranged such that the first $\operatorname{rank}(\boldsymbol{A}')$ columns of $\boldsymbol{A}'_{\mathcal{I}'_k}$ are linear independent for some $k\in[1,M]$, then we have

$$\sum_{k=1}^{M'}\operatorname{rank}(\boldsymbol{A}'_{\mathcal{I}'_k}) \ge N(N-(M-M')) \tag{88}$$

where $\boldsymbol{A}'_{\mathcal{I}'_k}$ is the submatrix of $\boldsymbol{A}'$ with N columns defined by $\mathcal{I}'_k$, i.e., $\boldsymbol{A}'_{\mathcal{I}'_k} \triangleq [A'_{j,i}]_{j\in[1,N],i\in\mathcal{I}'_k}$.

Proof: The sketch of the proofs for the above lemma is illustrated in Fig. 4(b). Given that there exists k such that the submatrix selected by the window has rank $r=N-(M-M')$ given by Lemma 3 and that the first r columns are linearly independent (the blue window in Fig.4(b)), the rank of the submatrix selected by the windows $\mathcal{I}'_{k-1},\dots,\mathcal{I}'_{k-(N-r)}$ (the red and brown windows in Fig.4(b)) is lower bounded by $r-1$. This lower bound keeps decreasing when the window slides go away from these positions, until it hits another lower bound $N-(M-N)=2N-M$ given by Lemma 3. With the help of Fig.4(b), a lower bound on the sum of the ranks of all the submatrices visited by the sliding window, can be obtained by counting the dots in the Figure. In fact, after some basic computations, it turns out that there are $N(N-(M-M'))$ dots. ■

Lemma 6. *Let $\boldsymbol{H}\in\mathbb{C}^{N\times M}$, $N\le M$, with $\boldsymbol{H}=\hat{\boldsymbol{H}}+\tilde{\boldsymbol{H}}$. If $\tilde{\boldsymbol{H}}$ has i.i.d. $\mathcal{N}_{\mathbb{C}}\left(0,\sigma^2\right)$ entries, then*

$$\mathbb{E}_{\tilde{\boldsymbol{H}}}\log\det(\boldsymbol{H}\boldsymbol{H}^{\mathsf{H}}) = (N-\operatorname{rank}(\hat{\boldsymbol{H}}))\log\sigma^2+O(1) \tag{89}$$

as σ^2 goes to 0.

Proof: The proof starts by rewriting the non-central Wishart Matrix $\boldsymbol{H}\boldsymbol{H}^{\mathsf{H}}$ with $\boldsymbol{H}=\hat{\boldsymbol{H}}+\tilde{\boldsymbol{H}}$. By SVD, the deterministic matrix can be decomposed as $\hat{\boldsymbol{H}}=\boldsymbol{U}\boldsymbol{\Lambda}\boldsymbol{V}^{\mathsf{H}}$, where $\boldsymbol{\Lambda}\in\mathbb{C}^{N\times M}$. Thus, we have

$$\begin{aligned}\boldsymbol{H}\boldsymbol{H}^{\mathsf{H}} &= \boldsymbol{U}\left(\boldsymbol{\Lambda}\boldsymbol{\Lambda}^{\mathsf{T}}+\boldsymbol{U}^{\mathsf{H}}\tilde{\boldsymbol{H}}\boldsymbol{V}\boldsymbol{\Lambda}^{\mathsf{T}}+\boldsymbol{\Lambda}\boldsymbol{V}^{\mathsf{H}}\tilde{\boldsymbol{H}}^{\mathsf{H}}\boldsymbol{U}+\boldsymbol{U}^{\mathsf{H}}\tilde{\boldsymbol{H}}\tilde{\boldsymbol{H}}^{\mathsf{H}}\boldsymbol{U}\right)\boldsymbol{U}^{\mathsf{H}} && (90)\\ &= \boldsymbol{U}\left(\boldsymbol{\Lambda}\boldsymbol{\Lambda}^{\mathsf{T}}+\sigma\boldsymbol{G}\boldsymbol{\Lambda}^{\mathsf{T}}+\sigma\boldsymbol{\Lambda}\boldsymbol{G}^{\mathsf{H}}+\sigma^2\boldsymbol{G}\boldsymbol{G}^{\mathsf{H}}\right)\boldsymbol{U}^{\mathsf{H}} && (91)\end{aligned}$$

where $\boldsymbol{G}\triangleq\frac{1}{\sigma}\boldsymbol{U}^{\mathsf{H}}\tilde{\boldsymbol{H}}\boldsymbol{V}\in\mathbb{C}^{N\times M}$ with each entry distributed as $\mathcal{N}_{\mathbb{C}}(0,1)$.

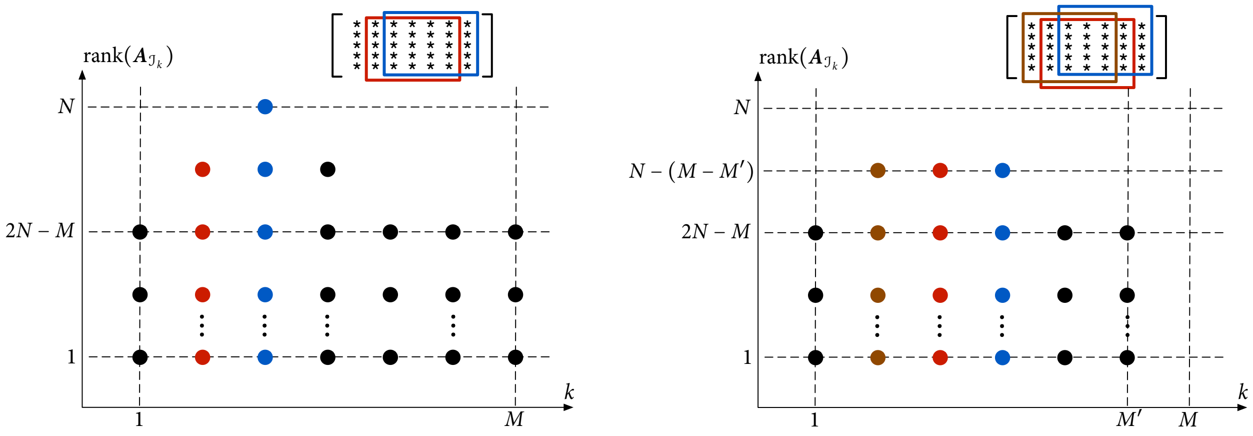

(a) An example for Lemma 4

(b) An example for Lemma 5

Fig. 4: Illustrations of the worst-case ranks of the submatrices from a sliding window. For each k, the number of vertical dots represents the rank of the submatrix $\boldsymbol{A}_{\mathcal{J}_k}$. In particular, the number of red (resp. blue) dots is the rank of the submatrix selected by the red (resp. blue) window. The sum of the ranks can be found by counting the number of dots.

Let $\boldsymbol{B} = \boldsymbol{G}\boldsymbol{G}^{\mathsf{H}}$ be divided into block format as $\boldsymbol{B} = \left[\begin{smallmatrix} \boldsymbol{B}_1 & \boldsymbol{B}_2 \\ \boldsymbol{B}_3 & \boldsymbol{B}_4 \end{smallmatrix}\right]$ with $\boldsymbol{B}_1 \in \mathbb{C}^{r\times r}$ and $\boldsymbol{B}_4 \in \mathbb{C}^{(N-r)\times(N-r)}$, where $r = \text{rank}(\hat{\boldsymbol{H}})$. Similarly, let $\boldsymbol{G} = \left[\begin{smallmatrix} \boldsymbol{G}_1 & \boldsymbol{G}_2 \\ \boldsymbol{G}_3 & \boldsymbol{G}_4 \end{smallmatrix}\right]$ with $\boldsymbol{G}_1 \in \mathbb{C}^{r\times r}$ and $\boldsymbol{G}_4 \in \mathbb{C}^{(N-r)\times(M-r)}$ and $\boldsymbol{\Lambda}_1 = \text{diag}\{\lambda_1, \cdots, \lambda_r\}$. Then, we have

$$\log\det(\boldsymbol{H}\boldsymbol{H}^{\mathsf{H}}) = \log\det(\boldsymbol{\Lambda}\boldsymbol{\Lambda}^{\mathsf{T}} + \sigma\boldsymbol{G}\boldsymbol{\Lambda}^{\mathsf{T}} + \sigma\boldsymbol{\Lambda}\boldsymbol{G}^{\mathsf{H}} + \sigma^2\boldsymbol{G}\boldsymbol{G}^{\mathsf{H}}) \tag{92}$$

$$= \log\det\left(\begin{bmatrix} \boldsymbol{\Lambda}_1^2 + \sigma\boldsymbol{G}_1\boldsymbol{\Lambda}_1 + \sigma^2\boldsymbol{B}_1 & \sigma\boldsymbol{\Lambda}_1\boldsymbol{G}_3^{\mathsf{H}} + \sigma^2\boldsymbol{B}_2 \\ \sigma\boldsymbol{G}_3\boldsymbol{\Lambda}_1 + \sigma^2\boldsymbol{B}_3 & \sigma^2\boldsymbol{B}_4 \end{bmatrix}\right) \tag{93}$$

$$= \log[\det(\sigma^2\boldsymbol{B}_4)\det(\boldsymbol{\Lambda}_1^2 + \sigma\boldsymbol{G}_1\boldsymbol{\Lambda}_1 + \sigma^2\boldsymbol{B}_1 - (\sigma\boldsymbol{\Lambda}_1\boldsymbol{G}_3^{\mathsf{H}} + \sigma^2\boldsymbol{B}_2)(\sigma^2\boldsymbol{B}_4)^{-1}\sigma\boldsymbol{G}_3\boldsymbol{\Lambda}_1 + \sigma^2\boldsymbol{B}_3)]$$

$$= \log\det(\sigma^2\boldsymbol{B}_4) + \log\det(\boldsymbol{X}_1 + \sigma\boldsymbol{X}_2 + \sigma^2\boldsymbol{X}_3) \tag{94}$$

$$= \log\det(\sigma^2\boldsymbol{B}_4) + \log\det(\boldsymbol{X}_1) + \log\det(\mathbf{I}_r + \sigma\boldsymbol{X}_1^{-1}\boldsymbol{X}_2 + \sigma^2\boldsymbol{X}_1^{-1}\boldsymbol{X}_3) \tag{95}$$

$$= \log\det(\sigma^2\boldsymbol{B}_4) + \log\det(\boldsymbol{X}_1) + O(1) \tag{96}$$

where

$$\boldsymbol{X}_1 = \boldsymbol{\Lambda}_1^2 + \boldsymbol{\Lambda}_1\boldsymbol{G}_3^{\mathsf{H}}\boldsymbol{B}_4^{-1}\boldsymbol{G}_3\boldsymbol{\Lambda}_1 \tag{97}$$

$$\boldsymbol{X}_2 = \boldsymbol{G}_1\boldsymbol{\Lambda}_1 - \boldsymbol{\Lambda}_1\boldsymbol{G}_3^{\mathsf{H}}\boldsymbol{B}_4^{-1}\boldsymbol{B}_3 - \boldsymbol{B}_2\boldsymbol{B}_4^{-1}\boldsymbol{G}_3\boldsymbol{\Lambda}_1 \tag{98}$$

$$\boldsymbol{X}_3 = \boldsymbol{B}_1 - \boldsymbol{B}_2\boldsymbol{B}_4^{-1}\boldsymbol{B}_3 \tag{99}$$

are all random matrices independent of σ, and the last line is according to the approximation of Taylor expansion for the determinant, i.e.,

$$\det(\mathbf{I}+\epsilon\boldsymbol{X}) = 1+\epsilon\mathrm{tr}(\boldsymbol{X})+O(\epsilon^2) = O(1) \tag{100}$$

when ϵ goes to 0.

Since $\boldsymbol{B}_4$ and $\boldsymbol{X}_1$ are made of Wishart matrices, both $\mathbb{E}_{\tilde{\boldsymbol{H}}}\log\det(\boldsymbol{B}_4)$ and $\mathbb{E}_{\tilde{\boldsymbol{H}}}\log\det(\boldsymbol{X}_1)$ exist. Hence, we have

$$\begin{aligned}\mathbb{E}_{\tilde{\boldsymbol{H}}}\log\det(\boldsymbol{H}\boldsymbol{H}^{\mathsf{H}}) &= \mathbb{E}_{\tilde{\boldsymbol{H}}}\log\det(\sigma^2\boldsymbol{B}_4)+\mathbb{E}_{\tilde{\boldsymbol{H}}}\log\det(\boldsymbol{X}_1)+O(1) &(101)\\ &= (N-r)\log(\sigma^2)+O(1) &(102)\end{aligned}$$

where $\boldsymbol{B}_4\in\mathbb{C}^{(N-r)\times(N-r)}$. This completes the proof.

■

B. Proof of Lemma 1

Let us define M' as the number of eigenvalues of $\boldsymbol{K}$ that are bounded from 0, i.e., $> O(1)$, as P grows large, and let $\boldsymbol{K}=\boldsymbol{V}\boldsymbol{\Lambda}\boldsymbol{V}^{\mathsf{H}}$ be the eigenvalue decomposition of $\boldsymbol{K}$. We first establish the following upper bound:

$$\begin{aligned}\det(\mathbf{I}+\boldsymbol{S}\boldsymbol{K}\boldsymbol{S}^{\mathsf{H}}) &= \det(\mathbf{I}+\boldsymbol{\Theta}\boldsymbol{\Lambda}\boldsymbol{\Theta}^{\mathsf{H}}) &(103)\\ &\le \det(\mathbf{I}+\boldsymbol{\Theta}'\boldsymbol{\Lambda}'(\boldsymbol{\Theta}')^{\mathsf{H}})+O(1) &(104)\\ &\le \det(\mathbf{I}+\|\boldsymbol{\Theta}'\|_{\mathrm{F}}^2\boldsymbol{\Lambda}')+O(1) &(105)\end{aligned}$$

where $\boldsymbol{\Theta}\triangleq\boldsymbol{S}\boldsymbol{V}$; $\boldsymbol{\Theta}'$ is a submatrix composed of the M' first columns of $\boldsymbol{\Theta}$ and $\boldsymbol{\Lambda}'$ is a diagonal matrix composed of the M' largest eigenvalues of $\boldsymbol{K}$. Therefore, we have

$$\begin{aligned}\mathbb{E}_{\tilde{\boldsymbol{S}}}\log\det(\mathbf{I}+\boldsymbol{S}\boldsymbol{K}\boldsymbol{S}^{\mathsf{H}}) &\le \log\det(\mathbf{I}+\boldsymbol{\Lambda}')+O(1) &(106)\\ &\le \log\det(\boldsymbol{\Lambda}')+O(1) &(107)\end{aligned}$$

where the last inequality holds since each eigenvalue of $\boldsymbol{\Lambda}'$ is bounded from 0.

Let $\boldsymbol{\Phi}\triangleq\boldsymbol{H}\boldsymbol{V}$, $\boldsymbol{\Phi}'\triangleq\hat{\boldsymbol{H}}\boldsymbol{V}$. Without loss of generality, we assume that the columns of $\boldsymbol{\Phi}$ and $\boldsymbol{\Phi}'$ are arranged such that the conditions in Lemma 4 and Lemma 5 are satisfied (i.e., $\mathrm{rank}(\boldsymbol{\Phi}_{\mathcal{J}})=N$, where $\mathcal{J}$ is the cyclic window with size N, and $\boldsymbol{\Phi}_{\mathcal{J}}$ is defined in the Appendix A), respectively. This also implies that the eigenvalues in $\boldsymbol{\Lambda}$ and $\boldsymbol{\Lambda}'$ are arranged accordingly. The lemma is solved for different values of M'.

1) Case $M'=M$: In this case, we have

$$\begin{aligned}\det(\mathbf{I}+\boldsymbol{H}\boldsymbol{K}\boldsymbol{H}^{\mathsf{H}}) &= \det(\mathbf{I}+\boldsymbol{\Phi}\boldsymbol{\Lambda}\boldsymbol{\Phi}^{\mathsf{H}}) &(108)\\ &= \sum_{\mathcal{J}\subseteq\{1,\ldots,N\}}\det(\boldsymbol{\Lambda}_{\mathcal{J}})\det(\boldsymbol{\Phi}_{\mathcal{J}}^{\mathsf{H}}\boldsymbol{\Phi}_{\mathcal{J}}) &(109)\\ &\ge \sum_{k=1}^{M}\det(\boldsymbol{\Phi}_{\mathcal{J}_k}^{\mathsf{H}}\boldsymbol{\Phi}_{\mathcal{J}_k})\det(\boldsymbol{\Lambda}_{\mathcal{J}_k}) &(110)\end{aligned}$$

where (109) is according to eq-(16) in [18], and the lower bound is obtained by only considering a sliding window of size N for all the possible sub-determinant. Further,

$$\log\det(\mathbf{I}+\boldsymbol{HKH}^{\mathsf{H}}) \geq \log\left(\sum_{k=1}^{M}\det(\boldsymbol{\Phi}_{\mathcal{J}_k}^{\mathsf{H}}\boldsymbol{\Phi}_{\mathcal{J}_k})\det(\boldsymbol{\Lambda}_{\mathcal{J}_k})\right) \tag{111}$$

$$\geq \log\left(\frac{1}{M}\sum_{k=1}^{M}\det(\boldsymbol{\Phi}_{\mathcal{J}_k}^{\mathsf{H}}\boldsymbol{\Phi}_{\mathcal{J}_k})\det(\boldsymbol{\Lambda}_{\mathcal{J}_k})\right) \tag{112}$$

$$\geq \frac{1}{M}\log\left(\prod_{k=1}^{M}\det(\boldsymbol{\Phi}_{\mathcal{J}_k}^{\mathsf{H}}\boldsymbol{\Phi}_{\mathcal{J}_k})\det(\boldsymbol{\Lambda}_{\mathcal{J}_k})\right) \tag{113}$$

$$= \frac{1}{M}\left(N\log\det(\boldsymbol{\Lambda}) + \sum_{k=1}^{M}\log\det(\boldsymbol{\Phi}_{\mathcal{J}_k}^{\mathsf{H}}\boldsymbol{\Phi}_{\mathcal{J}_k})\right) \tag{114}$$

where (111) is from (110); (113) is from the AM-GM inequality; the last equality is from the sliding window property $\prod_{k=1}^{M}\det(\boldsymbol{\Lambda}_{\mathcal{J}_k}) = \det(\boldsymbol{\Lambda})^{N}$. Finally, we have

$$\mathbb{E}_{\tilde{\boldsymbol{H}}}\log\det(\mathbf{I}+\boldsymbol{HKH}^{\mathsf{H}}) \geq \frac{1}{M}\left(N\log\det(\boldsymbol{\Lambda}) + \sum_{k=1}^{M}\mathbb{E}_{\tilde{\boldsymbol{H}}}\log\det(\boldsymbol{\Phi}_{\mathcal{J}_k}^{\mathsf{H}}\boldsymbol{\Phi}_{\mathcal{J}_k})\right) \tag{115}$$

$$\geq \frac{1}{M}\left(N\log\det(\boldsymbol{\Lambda}) + \log\sigma^2\sum_{k=1}^{M}(N-\operatorname{rank}(\hat{\boldsymbol{\Phi}}_{\mathcal{J}_k})) + O(1)\right) \tag{116}$$

$$\doteq \frac{1}{M}\left(N\log\det(\boldsymbol{\Lambda}) + \log\sigma^2\left(MN - \sum_{k=1}^{M}\operatorname{rank}(\hat{\boldsymbol{\Phi}}_{\mathcal{J}_k})\right)\right) \tag{117}$$

$$\geq \frac{N}{M}\left(\log\det(\boldsymbol{\Lambda}) + (M-N)\log\sigma^2\right) \tag{118}$$

where $\hat{\boldsymbol{\Phi}} \triangleq \hat{\boldsymbol{H}}\boldsymbol{V}$ and hence $\operatorname{rank}(\hat{\boldsymbol{\Phi}}) = \operatorname{rank}(\hat{\boldsymbol{H}})$; (116) is from Lemma 6; the last inequality is from Lemma 4. Combining (107) and (118), we have

$$N\,\mathbb{E}_{\tilde{\boldsymbol{S}}}\log\det(\mathbf{I}+\boldsymbol{SKS}^{\mathsf{H}}) - M\,\mathbb{E}_{\tilde{\boldsymbol{H}}}\log\det(\mathbf{I}+\boldsymbol{HKH}^{\mathsf{H}}) \leq -N(M-N)\log\sigma^2 + O(1). \tag{119}$$

2) Case $M > M' \geq N$: For this case, we can first get

$$\det(\mathbf{I}+\boldsymbol{HKH}^{\mathsf{H}}) = \det(\mathbf{I}+\boldsymbol{\Phi}\boldsymbol{\Lambda}\boldsymbol{\Phi}^{\mathsf{H}}) \tag{120}$$

$$\geq \det(\mathbf{I}+\boldsymbol{\Phi}'\boldsymbol{\Lambda}'(\boldsymbol{\Phi}')^{\mathsf{H}}). \tag{121}$$

Following the same foot steps as in the previous subsection, we can obtain

$$\mathbb{E}_{\tilde{\boldsymbol{H}}}\log\det(\mathbf{I}+\boldsymbol{HKH}^{\mathsf{H}}) \mathrel{\dot{\geq}} \frac{1}{M'}\left(N\log\det(\boldsymbol{\Lambda}') + \log\sigma^2\left(M'N - \sum_{k=1}^{M'}\operatorname{rank}(\hat{\boldsymbol{\Phi}}'_{\mathcal{J}'_k})\right)\right) \tag{122}$$

$$\geq \frac{N}{M'}\left(\log\det(\boldsymbol{\Lambda}') + (M-N)\log\sigma^2\right) \tag{123}$$

where the last inequality is from Lemma 5. Combining (107) and (123), we have

$$N\,\mathbb{E}_{\tilde{\boldsymbol{S}}}\log\det(\mathbf{I}+\boldsymbol{SKS}^{\mathsf{H}}) - M\,\mathbb{E}_{\tilde{\boldsymbol{H}}}\log\det(\mathbf{I}+\boldsymbol{HKH}^{\mathsf{H}}) \tag{124}$$

$$\leq N\,\mathbb{E}_{\tilde{\boldsymbol{S}}}\log\det(\mathbf{I}+\boldsymbol{SKS}^{\mathsf{H}})] - M'\,\mathbb{E}_{\tilde{\boldsymbol{H}}}\log\det(\mathbf{I}+\boldsymbol{HKH}^{\mathsf{H}})] \tag{125}$$

$$\leq -N(M-N)\log\sigma^2 + O(1). \tag{126}$$

3) Case $M' < N$: From (121) and given that $M' < N$, we have

$$\begin{aligned}
\mathbb{E}_{\tilde{\boldsymbol{H}}} \log\det(\mathbf{I} + \boldsymbol{HKH}^{\mathsf{H}}) &\geq \log\det(\boldsymbol{\Lambda}') + \log\sigma^2 \left(M' - \operatorname{rank}(\hat{\boldsymbol{\Phi}}')\right) && (127)\\
&\geq \log\det(\boldsymbol{\Lambda}') + \log\sigma^2 \left(M' - (N - (M - M'))\right) && (128)\\
&= \log\det(\boldsymbol{\Lambda}') + (M-N)\log\sigma^2 && (129)
\end{aligned}$$

where (128) is from $\log\sigma^2 \leq 0$ and $\operatorname{rank}(\hat{\boldsymbol{\Phi}}') \geq N - (M - M')$. Combining (107) and (129), we have

$$\begin{aligned}
&N\,\mathbb{E}_{\tilde{\boldsymbol{S}}} \log\det(\mathbf{I} + \boldsymbol{SKS}^{\mathsf{H}}) - M\,\mathbb{E}_{\tilde{\boldsymbol{H}}} \log\det(\mathbf{I} + \boldsymbol{HKH}^{\mathsf{H}}) && (130)\\
&\leq N\,\mathbb{E}_{\tilde{\boldsymbol{S}}} \log\det(\mathbf{I} + \boldsymbol{SKS}^{\mathsf{H}}) - N\,\mathbb{E}_{\tilde{\boldsymbol{H}}} \log\det(\mathbf{I} + \boldsymbol{HKH}^{\mathsf{H}}) && (131)\\
&\leq -N(M-N)\log\sigma^2 + O(1). && (132)
\end{aligned}$$

The above derivation considers all the possible relationships between M' and N, and therefore completes the proof.

C. Proof of Lemma 2

For the upper bound, we have

$$\begin{aligned}
\mathbb{E}_{\tilde{\boldsymbol{H}}} \log\det(\mathbf{I} + \boldsymbol{H}\boldsymbol{K}\boldsymbol{H}^{\mathsf{H}}) &= \mathbb{E}_{\tilde{\boldsymbol{H}}} \log\det(\mathbf{I} + \boldsymbol{U}_{\boldsymbol{H}}\boldsymbol{\Sigma}_{\boldsymbol{H}}\boldsymbol{V}_{\boldsymbol{H}}^{\mathsf{H}}\boldsymbol{K}\boldsymbol{V}_{\boldsymbol{H}}\boldsymbol{\Sigma}_{\boldsymbol{H}}\boldsymbol{U}_{\boldsymbol{H}}^{\mathsf{H}}) && (133)\\
&= \mathbb{E}_{\tilde{\boldsymbol{H}}} \log\det(\mathbf{I} + \boldsymbol{\Sigma}_{\boldsymbol{H}}^2\boldsymbol{V}_{\boldsymbol{H}}^{\mathsf{H}}\boldsymbol{K}\boldsymbol{V}_{\boldsymbol{H}}) && (134)\\
&\leq \mathbb{E}_{\tilde{\boldsymbol{H}}} \log\det(\mathbf{I} + \lambda_{\max}(\boldsymbol{\Sigma}_{\boldsymbol{H}}^2)\boldsymbol{V}_{\boldsymbol{H}}^{\mathsf{H}}\boldsymbol{K}\boldsymbol{V}_{\boldsymbol{H}}) && (135)\\
&= \sum_{i=1}^{N} \mathbb{E}_{\tilde{\boldsymbol{H}}} \log(1 + \lambda_{\max}(\boldsymbol{H}\boldsymbol{H}^{\mathsf{H}})\lambda_i(\boldsymbol{V}_{\boldsymbol{H}}^{\mathsf{H}}\boldsymbol{K}\boldsymbol{V}_{\boldsymbol{H}})) && (136)\\
&\leq \sum_{i=1}^{N} \mathbb{E}_{\tilde{\boldsymbol{H}}} \log(1 + \lambda_{\max}(\boldsymbol{H}\boldsymbol{H}^{\mathsf{H}})\lambda_i) && (137)\\
&\leq \sum_{i=1}^{N} \mathbb{E}_{\tilde{\boldsymbol{H}}} \log(1 + \|\boldsymbol{H}\|_{\mathrm{F}}^2\lambda_i) && (138)\\
&\leq \sum_{i=1}^{N} \mathbb{E}_{\tilde{\boldsymbol{H}}} \log(1 + (\|\hat{\boldsymbol{H}}\|_{\mathrm{F}}^2 + \|\tilde{\boldsymbol{H}}\|_{\mathrm{F}}^2)\lambda_i) && (139)\\
&\leq \sum_{i=1}^{N} \log(1 + (\|\hat{\boldsymbol{H}}\|_{\mathrm{F}}^2 + MN\sigma^2)\lambda_i) && (140)\\
&\leq \sum_{i=1}^{N} \log(1 + (\|\hat{\boldsymbol{H}}\|_{\mathrm{F}}^2 + MN)\lambda_i) + O(1) && (141)
\end{aligned}$$

where in (133), $\boldsymbol{H} = \boldsymbol{U}_{\boldsymbol{H}}\boldsymbol{\Sigma}_{\boldsymbol{H}}\boldsymbol{V}_{\boldsymbol{H}}^{\mathsf{H}}$ with $\boldsymbol{\Sigma}_{\boldsymbol{H}} \in \mathbb{C}^{N\times N}$ and $\boldsymbol{V}_{\boldsymbol{H}} \in \mathbb{C}^{M\times N}$; (134) comes from the equality $\det(\mathbf{I} + \boldsymbol{AB}) = \det(\mathbf{I} + \boldsymbol{BA})$; (137) is due to Poincare Separation Theorem [20] that $\lambda_i(\boldsymbol{V}_{\boldsymbol{H}}^{\mathsf{H}}\boldsymbol{K}\boldsymbol{V}_{\boldsymbol{H}}) \leq \lambda_i(\boldsymbol{K})$ for $i = 1, \cdots, N$; (138) is from the fact that $\|\boldsymbol{H}\|_2 \leq \|\boldsymbol{H}\|_{\mathrm{F}}$; (140) is obtained by applying Jensen's inequality to a concave function.

For the lower bound, we have

$$\begin{aligned}
\mathbb{E}_{\tilde{\boldsymbol{H}}} \log\det(\mathbf{I}+\boldsymbol{H}\boldsymbol{K}\boldsymbol{H}^{\mathsf{H}}) &\geq \mathbb{E}_{\tilde{\boldsymbol{H}}} N \log\left(1+\det(\boldsymbol{H}\boldsymbol{K}\boldsymbol{H}^{\mathsf{H}})^{1/N}\right) && (142)\\
&= \mathbb{E}_{\tilde{\boldsymbol{H}}} N \log\left(1+\exp\left(\frac{1}{N}\ln\det(\boldsymbol{H}\boldsymbol{K}\boldsymbol{H}^{\mathsf{H}})\right)\right) && (143)\\
&\geq N \log\left(1+\exp\left(\frac{1}{N}\mathbb{E}_{\tilde{\boldsymbol{H}}}\ln\det(\boldsymbol{H}\boldsymbol{K}\boldsymbol{H}^{\mathsf{H}})\right)\right) && (144)
\end{aligned}$$

where (142) comes from Minkowski's inequality and (144) is from Jensen's inequality by noticing that $\log(1+e^x)$ is a convex function in x. Hence, the expectation part can be simplified further as

$$\begin{aligned}
\mathbb{E}_{\tilde{\boldsymbol{H}}} \ln\det(\boldsymbol{H}\boldsymbol{K}\boldsymbol{H}^{\mathsf{H}}) &= \mathbb{E}_{\tilde{\boldsymbol{H}}} \ln\det\left(\boldsymbol{\Phi}\boldsymbol{\Lambda}\boldsymbol{\Phi}^{\mathsf{H}}\right) && (145)\\
&\geq \mathbb{E}_{\tilde{\boldsymbol{H}}} \ln\det\left(\boldsymbol{\Phi}'\boldsymbol{\Lambda}'\boldsymbol{\Phi}'^{\mathsf{H}}\right) && (146)\\
&= \ln\prod_{i=1}^{N}\lambda_i + \mathbb{E}_{\tilde{\boldsymbol{H}}} \ln\det\left(\boldsymbol{\Phi}'\boldsymbol{\Phi}'^{\mathsf{H}}\right) && (147)\\
&\geq \ln\prod_{i=1}^{N}\lambda_i + \mathbb{E}_{\tilde{\boldsymbol{H}}} \ln\det\left(\tilde{\boldsymbol{H}}\boldsymbol{V}'\boldsymbol{V}'^{\mathsf{H}}\tilde{\boldsymbol{H}}^{\mathsf{H}}\right) && (148)\\
&= \ln\prod_{i=1}^{N}\lambda_i + \mathbb{E}_{\tilde{\boldsymbol{H}}} \ln\det\left(\tilde{\boldsymbol{H}}'\tilde{\boldsymbol{H}}'^{\mathsf{H}}\right) && (149)\\
&= \ln\prod_{i=1}^{N}(\lambda_i\sigma^2) + \sum_{i=1}^{N}\psi(N-i+1) && (150)
\end{aligned}$$

where $\boldsymbol{\Phi}=\boldsymbol{H}\boldsymbol{V}\in\mathbb{C}^{N\times M}$ with $\boldsymbol{V}$ being the unitary matrix containing the eigenvectors of $\boldsymbol{K}$, i.e., $\boldsymbol{K}=\boldsymbol{V}\boldsymbol{\Lambda}\boldsymbol{V}^{\mathsf{H}}$ with $\boldsymbol{\Lambda}=\mathrm{diag}(\lambda_1,\cdots,\lambda_M)$; in (146), $\boldsymbol{\Phi}'=\boldsymbol{H}\boldsymbol{V}'\in\mathbb{C}^{N\times N}$ with $\boldsymbol{V}'$ being the first N columns of $\boldsymbol{V}$ where $\boldsymbol{\Lambda}'=\mathrm{diag}(\lambda_1,\cdots,\lambda_N)$ and $\boldsymbol{\Phi}\boldsymbol{\Lambda}\boldsymbol{\Phi}^{\mathsf{H}}\succeq\boldsymbol{\Phi}'\boldsymbol{\Lambda}'\boldsymbol{\Phi}'^{\mathsf{H}}$; (148) is due to the fact that the capacity of a Ricean fading channel is no less than that of a Rayleigh fading channel in all SNR region [21], by treating $\hat{\boldsymbol{H}}$ as the deterministic line-of-sight component; (149) is because of the i.i.d. assumption of $\tilde{\boldsymbol{H}}$, which is independent of $\boldsymbol{V}'$, and $\tilde{\boldsymbol{H}}'$ is an $N\times N$ matrix with each entry having the same distribution as that of $\tilde{\boldsymbol{H}}$; the last equation is according to the distribution assumption of $\tilde{\boldsymbol{H}}$ and obtained from [17].

By the definition $\zeta\triangleq\frac{1}{N}\sum_{i=1}^{N}\psi(N-i+1)$, we have

$$\begin{aligned}
N\log\left(1+\exp\left(\frac{1}{N}\mathbb{E}_{\tilde{\boldsymbol{H}}}\ln\det(\boldsymbol{H}\boldsymbol{K}\boldsymbol{H}^{\mathsf{H}})\right)\right) &\geq N\log\left(1+\exp\left(\frac{1}{N}\ln\prod_{i=1}^{N}(\lambda_i\sigma^2e^{\zeta})\right)\right) && (151)\\
&= N\log\left(1+\left(\prod_{i=1}^{N}(\lambda_i\sigma^2e^{\zeta})\right)^{\frac{1}{N}}\right) && (152)\\
&\geq N\frac{1}{N}\sum_{i=1}^{N}\left[\log(\lambda_i\sigma^2e^{\zeta})\right]^{+} && (153)\\
&\geq \sum_{i=1}^{N}\log(1+\lambda_i\sigma^2e^{\zeta})-N && (154)
\end{aligned}$$

$$= \sum_{i=1}^{N} \log(1 + \lambda_i \sigma^2 e^{\zeta}) + O(1) \tag{155}$$

where $(x)^+ \triangleq \max\{x, 0\}$ and last inequality due to the fact $(\log(x))^+ \geq \log(1 + x) - 1$.

The difference between upper and lower bounds can be further bounded as

$$\log(1 + (\|\hat{\boldsymbol{H}}\|_{\mathrm{F}}^2 + MN)\lambda_i) - \log(1 + \lambda_i \sigma^2 e^{\zeta}) \leq \log\left(\frac{1 + (\|\hat{\boldsymbol{H}}\|_{\mathrm{F}}^2 + MN)\lambda_i}{1 + \lambda_i \sigma^2 e^{\zeta}}\right) \tag{156}$$

$$\leq \log\left(1 + \frac{\|\hat{\boldsymbol{H}}\|_{\mathrm{F}}^2 + MN}{\sigma^2 e^{\zeta}}\right) \tag{157}$$

$$\leq -\log(\sigma^2) + O(1) \tag{158}$$

where the second inequality is due to the fact $\log\left(\frac{1+a}{1+b}\right) \leq \log\left(1 + \frac{a}{b}\right)$ and the last inequality is because both $(\|\hat{\boldsymbol{H}}\|_{\mathrm{F}}^2 + MN)$ and e^{ζ} are bounded. This completes the proof.

D. Generalized Achievable Schemes for Case B $(N < M < 2N)$

In this case, we demonstrate the DoF region stated in Theorem 3 is achievable, by showing the vertices

$$P_{B1} : (N, (M-N)\alpha) \quad P_{B2} : \left(\frac{MN + N^2\alpha}{M+N}, \frac{MN + (M^2 - N^2 - MN)\alpha}{M+N}\right) \tag{159}$$

and their counterparts (with swapped roles of two receivers) are all achievable.

Before proceeding further, we define

$$\boldsymbol{Q}_{ij}(t) \in \mathbb{C}^{M \times N} \subseteq \mathcal{R}\{\hat{\boldsymbol{H}}_{ij}(t)\}, \qquad \boldsymbol{Q}_{ij}^{\perp}(t) \in \mathbb{C}^{M \times (M-N)} \subseteq \mathcal{N}\{\hat{\boldsymbol{H}}_{ij}(t)\}, \tag{160a}$$

$$\boldsymbol{W}(t) \in \mathbb{C}^{M \times (M-N)} \subseteq \mathcal{R}\{\hat{\boldsymbol{H}}_{2[1:M-N]1}(t)\}, \qquad \boldsymbol{W}^{\perp}(t) \in \mathbb{C}^{M \times N} \subseteq \mathcal{N}\{\hat{\boldsymbol{H}}_{2[1:M-N]1}(t)\}. \tag{160b}$$

Note that the range and null spaces represent column space for notational conciseness. According to the definition of imperfect current CSIT, we have $\mathbb{E}\|\boldsymbol{H}_{ji}(t)\boldsymbol{Q}_{ji}^{\perp}(t)\|_{\mathrm{F}}^2 \sim P^{-\alpha}$ and $\mathbb{E}\|\boldsymbol{H}_{j[1:M-N]i}(t)\boldsymbol{W}^{\perp}(t)\|_{\mathrm{F}}^2 \sim P^{-\alpha}$.

Achievability of P_{B1}

This vertex can be achieved within one single slot by transmitting

$$\boldsymbol{x}_1 = \boldsymbol{Q}_{11}\boldsymbol{u}_c + \boldsymbol{W}^{\perp}\boldsymbol{u}_p, \quad \boldsymbol{x}_2 = \boldsymbol{Q}_{12}^{\perp}\boldsymbol{v}_p \tag{161}$$

where $\boldsymbol{u}_c \in \mathbb{C}^{N \times 1}$ with rate $N(1-\alpha)\log P$ is the common message decodable by both receivers but only desirable by Rx-1, and $\boldsymbol{u}_p \in \mathbb{C}^{N \times 1}$, $\boldsymbol{v}_p \in \mathbb{C}^{(M-N) \times 1}$ with respective rate of $N\alpha \log P$ and $(M-N)\alpha \log P$ are private messages that can be seen by its respective receiver, satisfying power constraints $\mathbb{E}\|\boldsymbol{u}_c\|^2 \leq P$ and $\mathbb{E}\|\boldsymbol{u}_p\|^2 = \mathbb{E}\|\boldsymbol{v}_p\|^2 \leq P^{\alpha}$. At the receiver side, we have

$$\boldsymbol{y}_1 = \underbrace{\boldsymbol{H}_{11}\boldsymbol{Q}_{11}\boldsymbol{u}_c}_{P} + \underbrace{\boldsymbol{H}_{11}\boldsymbol{W}^{\perp}\boldsymbol{u}_p}_{P^{\alpha}} + \underbrace{\boldsymbol{H}_{12}\boldsymbol{Q}_{12}^{\perp}\boldsymbol{v}_p}_{P^0}, \tag{162a}$$

$$\boldsymbol{y}_2 = \underbrace{\boldsymbol{H}_{21}\boldsymbol{Q}_{11}\boldsymbol{u}_c}_{P} + \underbrace{\boldsymbol{H}_{21}\boldsymbol{W}^{\perp}\boldsymbol{u}_p + \boldsymbol{H}_{22}\boldsymbol{Q}_{12}^{\perp}\boldsymbol{v}_p}_{P^{\alpha}}, \tag{162b}$$

$$\boldsymbol{y}_{2[1:M-N]} = \underbrace{\boldsymbol{H}_{2[1:M-N]1}\boldsymbol{Q}_{11}\boldsymbol{u}_c}_{P} + \underbrace{\boldsymbol{H}_{2[1:M-N]1}\boldsymbol{W}^{\perp}\boldsymbol{u}_p}_{P^0} + \underbrace{\boldsymbol{H}_{2[1:M-N]2}\boldsymbol{Q}_{12}^{\perp}\boldsymbol{v}_p}_{P^{\alpha}}, \tag{162c}$$

where $\boldsymbol{y}_{2[1:M-N]}$ is the first $M-N$ elements of $\boldsymbol{y}_2$. By first treating lower power terms as noise, both receiver can decode $N \times 1$ vector $\boldsymbol{u}_c$ from (162a) and (162b) provided N linearly independent equations, yielding $N(1-\alpha)$ DoF desired only by Rx-1. After that, the whole terms $\boldsymbol{H}_{11}\boldsymbol{Q}_{11}\boldsymbol{u}_c$ in (162a) and $\boldsymbol{H}_{2[1:M-N]1}\boldsymbol{Q}_{11}\boldsymbol{u}_c$ in (162c) can be reconstructed, and consequently subtracted from both received signals. Finally, the private messages $\boldsymbol{u}_p$ (resp. $\boldsymbol{v}_p$) can be recovered from the residual signal in (162a) at the Rx-1 [resp. in (162c) at the Rx-2], yielding $N\alpha$ [resp. $(M-N)\alpha$] DoF for Rx-1 (resp. Rx-2). We refer to this procedure as “successive decoding”. In the end, Rx-1 achieves total N DoF while Rx-2 obtains $(M-N)\alpha$ DoF. By exchanging the roles of two receivers, the DoF pair $((M-N)\alpha, N)$ can be achieved in a similar way.

Achivability of P_{B2}

It takes N slots in the first phase and M slots in the ensuing phase.

Phase-1: In this phase, N time slots are consumed to deliver MN symbols for each receiver. The transmitted signals in t-th time slot $(t = 1, \cdots, N)$ are given by

$$\boldsymbol{x}_1(t) = \begin{bmatrix}\boldsymbol{W}(t) & \boldsymbol{W}^{\perp}(t)\end{bmatrix}\boldsymbol{u}(t), \tag{163a}$$

$$\boldsymbol{x}_2(t) = \begin{bmatrix}\boldsymbol{Q}_{12}(t) & \boldsymbol{Q}_{12}^{\perp}(t)\end{bmatrix}\boldsymbol{v}(t), \tag{163b}$$

where $\boldsymbol{u}(t), \boldsymbol{v}(t) \in \mathbb{C}^{M\times 1}$. The received signals at both receivers can be given as

$$\boldsymbol{y}_1(t) = \boldsymbol{H}_{11}(t)\begin{bmatrix}\boldsymbol{W}(t) & \boldsymbol{W}^{\perp}(t)\end{bmatrix}\boldsymbol{u}(t) + \underbrace{\boldsymbol{H}_{12}(t)\begin{bmatrix}\boldsymbol{Q}_{12}(t) & \boldsymbol{Q}_{12}^{\perp}(t)\end{bmatrix}\boldsymbol{v}(t)}_{\boldsymbol{\eta}_t^1 \in \mathbb{C}^{N\times 1}}, \tag{164a}$$

$$\boldsymbol{y}_{2[1:M-N]}(t) = \underbrace{\boldsymbol{H}_{2[1:M-N]1}(t)\begin{bmatrix}\boldsymbol{W}(t) & \boldsymbol{W}^{\perp}(t)\end{bmatrix}\boldsymbol{u}(t)}_{\boldsymbol{\eta}^2_{t[1:M-N]} \in \mathbb{C}^{(M-N)\times 1}} + \boldsymbol{H}_{2[1:M-N]2}(t)\begin{bmatrix}\boldsymbol{Q}_{12}(t) & \boldsymbol{Q}_{12}^{\perp}(t)\end{bmatrix}\boldsymbol{v}(t), \tag{164b}$$

where only the first $M-N$ elements of $\boldsymbol{y}_2(t)$ are taken into account. By allocating $\boldsymbol{u}_{[1:M-N]} \sim P^{1-\alpha}$, $\boldsymbol{u}_{[M-N+1:M]} = P - (M-N)P^{1-\alpha} \sim P$, $\boldsymbol{v}_{[1:N]} \sim P^{1-\alpha}$, and $\boldsymbol{v}_{[N+1:M]} = P - NP^{1-\alpha} \sim P$, we have $\mathbb{E}\{\|\boldsymbol{\eta}_t^1\|^2\} \sim P^{1-\alpha}$ and $\mathbb{E}\{\|\boldsymbol{\eta}^2_{t[1:M-N]}\|^2\} \sim P^{1-\alpha}$, making it possible to compress them into $(1-\alpha)\log P$ bits for each element. Note that the efficient transmission rates are $(M-(M-N)\alpha)\log P$ for Tx-1 whereas $(M-N\alpha)\log P$ for Rx-2, respectively.

Before proceeding further, we concatenate all the interference terms as

$$\bar{\boldsymbol{\eta}}_k^1 = \begin{cases}\bar{\boldsymbol{\eta}}_k^1, & k = 1, \cdots, N \\ \boldsymbol{0}, & k = N+1, \cdots, M\end{cases}, \qquad \bar{\boldsymbol{\eta}}_k^2 = \begin{cases}\boldsymbol{0}, & k = 1, \cdots, N \\ \bar{\boldsymbol{\eta}}_{k-N}^2, & k = N+1, \cdots, M\end{cases} \tag{165}$$

where $\bar{\boldsymbol{\eta}}_k^1 \triangleq \begin{bmatrix}\eta_{1k}^1, \cdots & \eta_{Nk}^1\end{bmatrix}^{\mathsf{T}}, k = 1, \cdots, N$ and $\bar{\boldsymbol{\eta}}_k^2 \triangleq \begin{bmatrix}\eta_{1k}^2, \cdots & \eta_{Nk}^2\end{bmatrix}^{\mathsf{T}}, k = 1, \cdots, M-N$. Note that we abuse the notation of $\bar{\boldsymbol{\eta}}$ for simplicity.

Instead of forwarding the interference terms in an analog fashion [3, 5, 6], we quantize them first with source codebooks and then forward the indices of codewords to both receivers. A set of source codebooks $\{\mathcal{X}_{tk}^1, t =$

$1,\cdots,N, k=1,\cdots,M-N\}$ and $\{\mathcal{X}^2_{tk}, t=1,\cdots,N, k=1,\cdots,N\}$ with $(1-\alpha)\log P$ bits each are generated to represent the quantized elements of interference vectors at the Tx-1 and Tx-2, respectively. The codewords representing such quantized elements, denoted by $\hat{\eta}^2_{tk}$ and $\hat{\eta}^1_{tk}$, are chosen uniformly from $\{\mathcal{X}^1_{tk}\}$ and $\{\mathcal{X}^2_{tk}\}$.

Phase-2: The objective of Phase-2 is to forward the indices of quantized version $\hat{\boldsymbol{\eta}}^1_t$ and $\hat{\boldsymbol{\eta}}^2_{t[1:M-N]}$. Using Gaussian channel codebooks, the indices of $\hat{\boldsymbol{\eta}}^i_k$ are encoded one-to-one to $\boldsymbol{c}^i_k$, with rate of $N(1-\alpha)\log P$ bits satisfying power constraint $\mathbb{E}\|\boldsymbol{c}^i_k\|^2 \le P$. Then, $\{\boldsymbol{c}^i_k\}$ are forwarded as common messages to both receivers in the following M slots. It is worth noting that if $\hat{\boldsymbol{\eta}}^i_k = \mathbf{0}$, the corresponding transmitter keeps silent for it, i.e., $\boldsymbol{c}^i_k = \mathbf{0}$.

The transmitted signals at both transmitters are given by

$$\boldsymbol{x}_1(t) = \boldsymbol{\Phi}(t)\boldsymbol{c}^2_s + \boldsymbol{W}^{\perp}(t)\boldsymbol{u}_p(s), \tag{166a}$$

$$\boldsymbol{x}_2(t) = \boldsymbol{\Phi}(t)\boldsymbol{c}^1_s + \boldsymbol{Q}^{\perp}_{12}(t)\boldsymbol{v}_p(s), \tag{166b}$$

where $t=N+1,\cdots,M$, $s=t-N$, $\boldsymbol{\Phi}(t)\in\mathbb{C}^{M\times N}$ is a random matrix without lying in the null space of cross channels, $\boldsymbol{u}_p(s)\in\mathbb{C}^{N\times 1}$ and $\boldsymbol{v}_p(s)\in\mathbb{C}^{(M-N)\times 1}$ are private messages for Rx-1 and Rx-2 with rates $N\log P$ and $(M-N)\log P$, respectively, satisfying power constraint $\mathbb{E}\|\boldsymbol{u}_p(s)\|^2 = \mathbb{E}\|\boldsymbol{v}_p(s)\|^2 \le P^{\alpha}$.

The received signals at the receivers are given by

$$\boldsymbol{y}_1(t) = \underbrace{\boldsymbol{H}_{11}(t)\boldsymbol{\Phi}(t)\boldsymbol{c}^2_s + \boldsymbol{H}_{12}(t)\boldsymbol{\Phi}(t)\boldsymbol{c}^1_s}_{P} + \underbrace{\boldsymbol{H}_{11}(t)\boldsymbol{W}^{\perp}(t)\boldsymbol{u}_p(s)}_{P^{\alpha}} + \underbrace{\boldsymbol{H}_{12}(t)\boldsymbol{Q}^{\perp}_{12}(t)\boldsymbol{v}_p(s)}_{P^0}, \tag{167a}$$

$$\boldsymbol{y}_2(t) = \underbrace{\boldsymbol{H}_{21}(t)\boldsymbol{\Phi}(t)\boldsymbol{c}^2_s + \boldsymbol{H}_{22}(t)\boldsymbol{\Phi}(t)\boldsymbol{c}^1_s}_{P} + \underbrace{\boldsymbol{H}_{21}(t)\boldsymbol{W}^{\perp}(t)\boldsymbol{u}_p(s) + \boldsymbol{H}_{22}(t)\boldsymbol{Q}^{\perp}_{12}(t)\boldsymbol{v}_p(s)}_{P^{\alpha}}, \tag{167b}$$

$$\begin{aligned}\boldsymbol{y}_{2[1:M-N]}(t) = {} & \underbrace{\boldsymbol{H}_{2[1:M-N]1}(t)\boldsymbol{\Phi}(t)\boldsymbol{c}^2_s + \boldsymbol{H}_{2[1:M-N]2}(t)\boldsymbol{\Phi}(t)\boldsymbol{c}^1_s}_{P} \\ & + \underbrace{\boldsymbol{H}_{2[1:M-N]1}(t)\boldsymbol{W}^{\perp}(t)\boldsymbol{u}_p(s)}_{P^0} + \underbrace{\boldsymbol{H}_{2[1:M-N]2}(t)\boldsymbol{Q}^{\perp}_{12}(t)\boldsymbol{v}_p(s)}_{P^{\alpha}}.\end{aligned} \tag{167c}$$

Note that either $\boldsymbol{c}^1_s$ or $\boldsymbol{c}^2_s$ is $\mathbf{0}$ in each equation according to (165). By treating other terms as noise, $\boldsymbol{c}^i_s$ can be decoded from (167a)-(167b) at both receivers provided the compression rate is not greater than $N(1-\alpha)\log P$. After that, the terms containing $\boldsymbol{c}^i_s$ is reconstructed and subtracted from the received signals in (167b) and (167c) to recover the private messages (i.e., $\boldsymbol{u}_p(s)$ and $\boldsymbol{v}_p(s)$). With N (resp. $M-N$) linearly independent equations, the private messages $\boldsymbol{u}_p(s)$ (resp. $\boldsymbol{v}_p(s)$) with total N (resp. $M-N$) symbols are retrievable at Rx-1 (resp. Rx-2) as long as the power constraints are satisfied, yielding additional $N\alpha$ and $(M-N)\alpha$ DoF for Rx-1 and Rx-2 respectively in each slot. In the end, the codeword vector $\boldsymbol{c}^i_s$ can be all recovered (and in turn $\hat{\boldsymbol{\eta}}^i_k$) at both receivers, serving to cancel the overheard interference as well as to provide additional linearly independent equations for $\boldsymbol{u}(t)$ and $\boldsymbol{v}(t)$. With sufficient linearly independent equations, the vectors $\boldsymbol{u}(t)$ and $\boldsymbol{v}(t)$ are both recoverable with high probability at its respective receiver. Hence, we have the achievable DoF pair

$$d_1 = \frac{N(M-(M-N)\alpha) + MN\alpha}{M+N} = \frac{MN + N^2\alpha}{M+N}, \tag{168a}$$

$$d_2 = \frac{N(M-N\alpha) + M(M-N)\alpha}{M+N} = \frac{MN + (M^2 - N^2 - MN)\alpha}{M+N}. \tag{168b}$$

By swapping the roles of Rx-1 and Rx-2, the counterpart point is also achievable.

E. Generalized Achievable Schemes for Case C ($M \geq 2N$)

As stated before, we consider $M = 2N$ case since additional transmit antennas do not increase DoF [2, 5]. In this case, we demonstrate the outer bound in Theorem 1 is tight (as Theorem 2 claimed), where the vertices

$$P_{C1} : (N, N\alpha), \quad P_{C2} : \left(\frac{N(2+\alpha)}{3}, \frac{N(2+\alpha)}{3} \right) \tag{169}$$

and their counterparts (with exchanged roles of both receivers) are all achievable. Note that this case coincides with the MISO case except the multiplied DoF by N.

Following the similar definition, we have

$$\boldsymbol{Q}_{ij}(t) \in \mathbb{C}^{2N \times N} \subseteq \mathcal{R}\{\hat{\boldsymbol{H}}_{ij}(t)\}, \qquad \boldsymbol{Q}_{ij}^{\perp}(t) \in \mathbb{C}^{2N \times N} \subseteq \mathcal{N}\{\hat{\boldsymbol{H}}_{ij}(t)\} \tag{170}$$

where $\mathbb{E}\|\boldsymbol{H}_{ji}(t)\boldsymbol{Q}_{ji}^{\perp}(t)\|_{\mathrm{F}}^2 \sim P^{-\alpha}$.

Achievability of P_{C1}

This vertex can be achieved within one single slot. The transmission can be given by

$$\boldsymbol{x}_1 = \boldsymbol{Q}_{11}\boldsymbol{u}_c + \boldsymbol{Q}_{21}^{\perp}\boldsymbol{u}_p, \quad \boldsymbol{x}_2 = \boldsymbol{Q}_{12}^{\perp}\boldsymbol{v}_p \tag{171}$$

where $\boldsymbol{u}_c \in \mathbb{C}^{N \times 1}$, $\boldsymbol{u}_p \in \mathbb{C}^{N \times 1}$ and $\boldsymbol{v}_p \in \mathbb{C}^{N \times 1}$. The transmitted symbols are assumed to satisfy the power constraints $\mathbb{E}\|\boldsymbol{u}_c\|^2 \leq P$ and rate $N(1-\alpha)\log P$, whereas $\mathbb{E}\|\boldsymbol{u}_p\|^2 = \mathbb{E}\|\boldsymbol{v}_p\|^2 \leq P^{\alpha}$ and rate $N\alpha \log P$. Although the symbol $\boldsymbol{u}_c$ is decodable by both receivers and hence referred to as a common message, it is only desirable by Rx-1. On the other hand, we refer to $\boldsymbol{u}_p$, $\boldsymbol{v}_p$ as the private messages which can only be seen and decoded by their corresponding receivers. At the receiver side, we have

$$\boldsymbol{y}_1 = \underbrace{\boldsymbol{H}_{11}\boldsymbol{Q}_{11}\boldsymbol{u}_c}_{P} + \underbrace{\boldsymbol{H}_{11}\boldsymbol{Q}_{21}^{\perp}\boldsymbol{u}_p}_{P^{\alpha}} + \underbrace{\boldsymbol{H}_{12}\boldsymbol{Q}_{12}^{\perp}\boldsymbol{v}_p}_{P^{0}}, \tag{172a}$$

$$\boldsymbol{y}_2 = \underbrace{\boldsymbol{H}_{21}\boldsymbol{Q}_{11}\boldsymbol{u}_c}_{P} + \underbrace{\boldsymbol{H}_{21}\boldsymbol{Q}_{21}^{\perp}\boldsymbol{u}_p}_{P^{0}} + \underbrace{\boldsymbol{H}_{22}\boldsymbol{Q}_{12}^{\perp}\boldsymbol{v}_p}_{P^{\alpha}}. \tag{172b}$$

By successive decoding, the two receivers decode common message $\boldsymbol{u}_c$ by treating other terms as noise. Then, subtracting the terms with $\boldsymbol{u}_c$, two receivers can decode their own private messages successfully, yielding total N and $N\alpha$ DoF for Rx-1 and Rx-2, respectively.

Achievability of P_{C2}

To achieve such a vertex, three time slots are sufficient.

Slot-1: The transmitted signals from both transmitters are given by

$$\boldsymbol{x}_1(1) = \begin{bmatrix}\boldsymbol{Q}_{21}(1) & \boldsymbol{Q}_{21}^{\perp}(1)\end{bmatrix} \boldsymbol{u}(1), \tag{173a}$$

$$\boldsymbol{x}_2(1) = \begin{bmatrix}\boldsymbol{Q}_{12}(1) & \boldsymbol{Q}_{12}^{\perp}(1)\end{bmatrix} \boldsymbol{v}(1), \tag{173b}$$

where $\boldsymbol{u}(1) \triangleq \begin{bmatrix}\boldsymbol{u}_1^{\mathsf{T}}(1) & \boldsymbol{u}_2^{\mathsf{T}}(1)\end{bmatrix}^{\mathsf{T}}$, $\boldsymbol{v}(1) \triangleq \begin{bmatrix}\boldsymbol{v}_1^{\mathsf{T}}(1) & \boldsymbol{v}_2^{\mathsf{T}}(1)\end{bmatrix}^{\mathsf{T}}$ with $\boldsymbol{u}_i(1), \boldsymbol{v}_i(1) \in \mathbb{C}^{N\times 1}$.

At both receivers, we have

$$\boldsymbol{y}_1(1) = \boldsymbol{H}_{11}(1) \begin{bmatrix}\boldsymbol{Q}_{21}(1) & \boldsymbol{Q}_{21}^{\perp}(1)\end{bmatrix} \boldsymbol{u}(1) + \underbrace{\boldsymbol{H}_{12}(1) \begin{bmatrix}\boldsymbol{Q}_{12}(1) & \boldsymbol{Q}_{12}^{\perp}(1)\end{bmatrix} \boldsymbol{v}(1)}_{\boldsymbol{\eta}_1 \in \mathbb{C}^{N\times 1}}, \tag{174a}$$

$$\boldsymbol{y}_2(1) = \underbrace{\boldsymbol{H}_{21}(1) \begin{bmatrix}\boldsymbol{Q}_{21}(1) & \boldsymbol{Q}_{21}^{\perp}(1)\end{bmatrix} \boldsymbol{u}(1)}_{\boldsymbol{\eta}_2 \in \mathbb{C}^{N\times 1}} + \boldsymbol{H}_{22}(1) \begin{bmatrix}\boldsymbol{Q}_{12}(1) & \boldsymbol{Q}_{12}^{\perp}(1)\end{bmatrix} \boldsymbol{v}(1). \tag{174b}$$

By balancing the allocated power among those vectors, i.e., $\mathbb{E}\|\boldsymbol{u}_1(1)\|^2 = \mathbb{E}\|\boldsymbol{v}_1(1)\|^2 \sim P^{1-\alpha}$ and $\mathbb{E}\|\boldsymbol{u}_2(1)\|^2 = \mathbb{E}\|\boldsymbol{v}_2(1)\|^2 = P - NP^{1-\alpha} \sim P$, we approximate the total power of interference vectors as $\mathbb{E}\|\boldsymbol{\eta}_1\|^2 \sim P^{1-\alpha}$ and $\mathbb{E}\|\boldsymbol{\eta}_2\|^2 \sim P^{1-\alpha}$. A set of source codebooks $\{\mathcal{X}_{1i}, \mathcal{X}_{2i}, i = 1, \cdots, N\}$ with size $(1-\alpha)\log P$ bits each are generated to represent the quantized elements of the interference vectors $\boldsymbol{\eta}_2$ and $\boldsymbol{\eta}_1$ at the Tx-1 and Tx-2, respectively. The codewords representing the elements of $\boldsymbol{\eta}_2$ and $\boldsymbol{\eta}_1$ are chosen uniformly from $\{\mathcal{X}_{1i}\}$ and $\{\mathcal{X}_{2i}\}$ and concatenated as $\hat{\boldsymbol{\eta}}_2$ and $\hat{\boldsymbol{\eta}}_1$, respectively. Then, the indices of $\hat{\boldsymbol{\eta}}_i$ are encoded to $\boldsymbol{c}_i$ with rate $N(1-\alpha)\log P$ and power constraint $\mathbb{E}\|\boldsymbol{c}_i\|^2 \le P$ using a Gaussian channel codebook, and then forwarded as common messages to both receivers in the following two slots.

Slot-2 & Slot-3: These two slots are similar. The objective of the Slot-2 (resp. Slot-3) is to convey the coded common message $\boldsymbol{c}_2$ (resp. $\boldsymbol{c}_1$) carrying the information of $\hat{\boldsymbol{\eta}}_2$ (resp. $\hat{\boldsymbol{\eta}}_1$), together with a new symbol vector at the Tx-1 (resp. Tx-2), while only a new symbol vector is sent at the Tx-2 (resp. Tx-1). The transmitted signals in two slots are

$$\text{Slot-2:} \quad \begin{aligned} \boldsymbol{x}_1(2) &= \boldsymbol{Q}_{21}(2)\boldsymbol{c}_2 + \boldsymbol{Q}_{21}^{\perp}(2)\boldsymbol{u}(2) \\ \boldsymbol{x}_2(2) &= \boldsymbol{Q}_{12}^{\perp}(2)\boldsymbol{v}(2) \end{aligned} \tag{175a}$$

$$\text{Slot-3:} \quad \begin{aligned} \boldsymbol{x}_1(3) &= \boldsymbol{Q}_{21}^{\perp}(3)\boldsymbol{u}(3) \\ \boldsymbol{x}_2(3) &= \boldsymbol{Q}_{12}(3)\boldsymbol{c}_1 + \boldsymbol{Q}_{12}^{\perp}(3)\boldsymbol{v}(3) \end{aligned} \tag{175b}$$

where $\boldsymbol{u}(2), \boldsymbol{v}(2), \boldsymbol{u}(3), \boldsymbol{v}(3) \in \mathbb{C}^{N\times 1}$ with rate $N\alpha\log P$ each, satisfying $\mathbb{E}\|\boldsymbol{u}(2)\|^2 = \mathbb{E}\|\boldsymbol{u}(3)\|^2 \le P^{\alpha}$ and $\mathbb{E}\|\boldsymbol{v}(2)\|^2 = \mathbb{E}\|\boldsymbol{v}(3)\|^2 \le P^{\alpha}$.

In Slot-2, the received signals are give by (the received signals in Slot-3 can be similarly obtained)

$$\boldsymbol{y}_1(2) = \underbrace{\boldsymbol{H}_{11}(2)\boldsymbol{Q}_{21}(2)\boldsymbol{c}_2}_{P} + \underbrace{\boldsymbol{H}_{11}(2)\boldsymbol{Q}_{21}^{\perp}(2)\boldsymbol{u}(2)}_{P^{\alpha}} + \underbrace{\boldsymbol{H}_{12}(2)\boldsymbol{Q}_{12}^{\perp}(2)\boldsymbol{v}(2)}_{P^{0}}, \tag{176a}$$

$$\boldsymbol{y}_2(2) = \underbrace{\boldsymbol{H}_{21}(2)\boldsymbol{Q}_{21}(2)\boldsymbol{c}_2}_{P} + \underbrace{\boldsymbol{H}_{21}(2)\boldsymbol{Q}_{21}^{\perp}(2)\boldsymbol{u}(2)}_{P^{0}} + \underbrace{\boldsymbol{H}_{22}(2)\boldsymbol{Q}_{12}^{\perp}(2)\boldsymbol{v}(2)}_{P^{\alpha}}. \tag{176b}$$

By treating other terms as noise, $N \times 1$ vector $\boldsymbol{c}_2$ is retrievable at both receivers with high probability provided N linearly independent equations. After that, $\boldsymbol{u}(2)$ and $\boldsymbol{v}(2)$ are also recoverable from N linear equations at the Rx-1 and Rx-2 by subtracting the terms with $\boldsymbol{c}_2$ from the received signals. The same strategy applies to Slot-3.

In the end, $N \times 1$ codeword vector $\boldsymbol{c}_1$ and $\boldsymbol{c}_2$ can be all recovered (and in turn $\hat{\boldsymbol{\eta}}_1$ and $\hat{\boldsymbol{\eta}}_2$) at both receivers, serving to cancel the overheard interference as well as to provide additional linearly independent equations for $\boldsymbol{v}(1)$ and $\boldsymbol{u}(1)$, respectively. With $2N$ linearly independent equations, the $2N \times 1$ vectors $\boldsymbol{u}(1)$ and $\boldsymbol{v}(1)$ are both recoverable with high probability at its respective receiver. Hence, the total $N(2+\alpha)$ DoF for each receiver is achieved within three time slots, and in turn P_{C2} is achievable by symmetry.

ACKNOWLEDGEMENT

The first author would like to thank Paul de Kerret for his help on reviewing the paper and providing the idea of the proof for Lemma 6.

REFERENCES

[1] H. Weingarten, Y. Steinberg, and S. Shamai (Shitz). "The capacity region of the Gaussian multiple-input multiple-output broadcast channel," *IEEE Trans. Inf. Theory*, vol. 52, no. 9, pp. 3936–3964, Sep. 2006.

[2] S. A. Jafar and M. Fakhereddin, "Degrees of freedom for the MIMO interference channel," *IEEE Trans. Inf. Theory*, vol. 53, pp. 2637–2642, Jul. 2007.

[3] M. Maddah-Ali and D. Tse, "Completely stale transmitter channel state information is still very useful," *in Proc. of Allerton Conference*, Monticello, IL, Oct. 2010, Arxiv preprint arXiv:1010.1499.

[4] C. S. Vaze and M. K. Varanasi, "The degrees of freedom region of two-user and certain three-user MIMO broadcast channel with delayed CSI," Dec. 2010, *submitted to IEEE Trans. Inf. Theory*, available on arXiv:1101.0306v2.

[5] C. S. Vaze, M. K. Varanasi, "The degrees of freedom region and interference alignment for the MIMO interference channel with delayed CSIT," *IEEE Trans. Inf. Theory*, vol. 58, no. 7, pp. 4396–4417, Jul. 2012.

[6] A. Ghasemi, A. Motahari, and A. Khandani, "Interference alignment for the MIMO interference channel with delyed local CSIT," Arxiv preprint arXiv: 1102.5673, Feb. 2011.

[7] Y. Zhu and D. Guo, "The degrees of freedom of isotropic MIMO interference channels without state information at transmitters," *IEEE Trans. Inf. Theory*, vol. 58, no. 1, pp. 341–352, Jan. 2012.

[8] C. Huang, S. A. Jafar, S. Shamai, and S. Vishwanath, "On degrees of freedom region of MIMO networks without CSIT," *IEEE Trans. Inf. Theory*, vol. 58, no. 2, pp. 849–857, Feb. 2012.

[9] C. Vaze and M. Varanasi, "The degrees of freedom regions of MIMO broadcast, interference, and cognitive radio channels with no CSIT," *IEEE Trans. Inf. Theory*, vol. 58, no. 8, pp. 5354–5374, Aug. 2012.

[10] M. Kobayashi, S. Yang, D. Gesbert, X. Yi, "On the degrees of freedom of time correlated MISO broadcast channel with delayed CSIT," *in Proc. IEEE International Symposium on Information Theory (ISIT)*, Cambridge, MA, USA, Jul. 2012, Arxiv preprint arXiv:1202.1909.

[11] S. Yang, M. Kobayashi, D. Gesbert, X. Yi, "Degrees of freedom of time correlated MISO broadcast channel with delayed CSIT," *to appear in IEEE Trans. Inf. Theory*, Arxiv preprint arXiv:1203.2550, Mar. 2012.

[12] T. Gou and S. A. Jafar, "Optimal use of current and outdated channel state information–Degrees of freedom of the MISO BC with mixed CSIT," *IEEE Communications Letters*, vol. 16, no. 7 , Jul. 2012, pp. 1084–1087.

[13] X. Yi, D. Gesbert, S. Yang, M. Kobayashi, "On the DoF of the multiple-antenna time correlated interference channel with delayed CSIT," *to appear in Proc. Asilomar Conference on Signals and Systems* (Invited Paper), Pacific Grove, CA, USA, Nov. 2012. Arxiv preprint arXiv: 1204.3046v2 (full version).

[14] G. Caire, N. Jindal, M. Kobayashi, and N. Ravindran, "Multiuser MIMO achievable rates with downlink training and channel state feedback," *IEEE Trans. Inf. Theory*, vol. 56, no. 6, pp. 2845–2866, Jun. 2010.

[15] M. Kobayashi, and G. Caire, “On the net DoF comparison between ZF and MAT over time-varying MISO broadcast channels,” *in Proc. IEEE International Symposium on Information Theory (ISIT)*, Cambridge, MA, USA, Jul. 2012

[16] T. Liu and P. Viswanath, “An extremal inequality motivated by multiterminal information-theoretic problems,” *IEEE Trans. Inf. Theory*, vol. 53, no. 5, pp. 1839–1851, May 2007.

[17] O. Oyman, R. U. Nabar, H. Bolcskei, and A. J. Paulraj, “Characterizing the statistical properties of mutual information in MIMO channels,” *IEEE Trans. Sig. Proc.*, vol. 51, no. 11, Nov. 2003.

[18] S. Jin, X. Q. Gao, and X. H. You, “On the ergodic capacity of rank-1 Ricean fading MIMO channels,” *IEEE Trans. Inform. Theory*, vol. 53, no. 2, pp. 502–517, 2007.

[19] T. Cover and J. Thomas, *Elements of Information Theory*, New York: Wiley, 2006.

[20] D. Palomar, J. Cioffi, and M. Lagunas, “Uniform power allocation in MIMO channels: A game-theoretic approach,” *IEEE Trans. Inf. Theory*, vol. 49, no. 7, pp. 1707–1727, July 2003.

[21] D. Hosli, Y.-H. Kim, and A. Lapidoth, “Monotonicity results for coherent MIMO Rician channels,” *IEEE Trans. Inf. Theory*, vol. 51, no. 12, pp. 4334–4339, Dec. 2005.